Antibiotics promote intestinal growth of carbapenem-resistant *Enterobacteriaceae* by enriching nutrients and depleting microbial metabolites

Alexander Y. G. Yip[1], Olivia G. King[2], Oleksii Omelchenko[1], Sanjana Kurkimat[1], Victoria Horrocks[1], Phoebe Mostyn[1], Nathan Danckert[3], Rohma Ghani[3,4], Giovanni Satta[5], Frances J. Davies[4], Thomas B. Clarke[2], Benjamin H. Mullish[3,6], Julian R. Marchesi[3], Julie A. K. McDonald[1]*

Affiliations:

[1] Department of Life Sciences, Imperial College London, London SW7 2AZ, United Kingdom.

[2] Department of Infectious Disease, Imperial College London, London SW7 2AZ, United Kingdom.

[3] Division of Digestive Diseases, Department of Metabolism, Digestion and Reproduction, Faculty of Medicine, St Mary's Hospital Campus, Imperial College London, London, United Kingdom.

[4] Department of Infectious Disease, Imperial College Healthcare NHS Trust, London, United Kingdom.

[5] UCL Centre for Clinical Microbiology, University College London, United Kingdom.

[6] Departments of Gastroenterology and Hepatology, St Mary's Hospital, Imperial College Healthcare NHS Trust, Paddington, London, UK

* Corresponding author

Correspondence:

Dr. Julie A. K. McDonald

Imperial College London

Room 1.44, Flowers Building

Exhibition Road

London SW7 2AZ

Email: julie.mcdonald@imperial.ac.uk

Telephone: +44 (0)20 7594 5247

Acknowledgements: This work was supported by funding awarded to JAKM: a Medical Research Council (MRC) New Investigator Research Grant (MR/W025655/1), a Wellcome Trust Institutional Strategic Support Fund Springboard Fellowship, and startup funds from the Department of Life Sciences at Imperial College London. FJD received funding from the Medical Research Council (MRC) Clinical Academic Research Partnership Scheme. TBC received funding from a UKRI Impact Accelerator Award (MR/X502959/1). BHM is the recipient of an NIHR Academic Clinical Lectureship (CL-2019-21-002). The Division of Digestive Diseases received financial and infrastructure support from the National Institute for Health Research (NIHR) Imperial Biomedical Research Centre (BRC) based at Imperial College Healthcare NHS Trust and Imperial College London.

Author contributions:

Alexander Y. G. Yip, MRes = formal analysis: equal; investigation: lead; methodology: equal; visualisation: equal; writing – review & editing: supporting

Olivia G. King, MSc = investigation: supporting; writing – review & editing: supporting

Oleksii Omelchenko, MRes = formal analysis: supporting; investigation: supporting

Sanjana Kurkimat, MSc = formal analysis: supporting; investigation: supporting

Victoria Horrocks, PhD = formal analysis: supporting; investigation: supporting; writing – review & editing: supporting

Phoebe Mostyn, MRes = formal analysis: supporting; investigation: supporting

Nathan Danckert, PhD = investigation: supporting

Rohma Ghani, MB BS = resources: supporting, writing – review & editing: supporting

Giovanni Satta, PhD = resources: supporting, writing – review & editing: supporting

Frances J. Davies, PhD = resources: supporting; writing – review & editing: supporting

Thomas B. Clarke, PhD = investigation: supporting; methodology: supporting; writing – review & editing: supporting

Benjamin H. Mullish, PhD = resources: supporting; writing – review & editing: supporting

Julian R. Marchesi, PhD = resources: supporting; writing – review & editing: supporting

Julie A. K. McDonald, PhD = conceptualisation: lead; data curation: lead; formal analysis: equal; funding acquisition: lead; methodology: equal; project administration: lead; resources: lead; supervision: lead; visualisation: equal; writing – original draft: lead; writing – review & editing: lead

Disclosures: JAKM, AYGY, and OGK have filed a patent application related to this work (patent application number 2217266.2). BHM received consultancy fees from Finch Therapeutics Group, Ferring Pharmaceuticals, and Summit Therapeutics, outside of the submitted work. JRM received consultancy fees from EnteroBiotix Ltd. and Cultech Ltd, outside of the submitted work. All other authors disclose no conflicts.

Abbreviations: ^{1}H-NMR, proton nuclear magnetic resonance; AMiGA, Analysis of Microbial Growth Assays; ANOVA, analysis of variance; BCFA, branched chain fatty acid; CAZ, ceftazidime; CFU, colony forming units; CIP, ciprofloxacin; CRE, carbapenem-resistant *Enterobacteriaceae*; CRO, ceftriaxone; CTX, cefotaxime; ETP, ertapenem; FDR, false discovery rate; IPM, imipenem/cilastatin; LB, Luria broth; LOD, limit of detection; MEM, meropenem; NDM-1, New Delhi Metallo-β-lactamase 1; OD_{600}, optical density at 600 nm; PBS, phosphate-buffered saline; PCR, polymerase chain reaction; rCCA, regularised canonical correlation analysis; SCFA, short chain fatty acid; TSP, 3-(Trimethylsilyl)propionic-2,2,3,3-d4 acid sodium salt; TZP, piperacillin/tazobactam

Keywords: gut microbiota; nutrient competition; metabolite inhibition; colonisation resistance

ABSTRACT

The intestine is the primary colonisation site for carbapenem-resistant *Enterobacteriaceae* (CRE) and serves as a reservoir of CRE that cause invasive infections (e.g. bloodstream infections). Antibiotics disrupt colonisation resistance mediated by the gut microbiota, promoting the expansion of CRE within the intestine. We used *ex vivo* faecal cultures to measure the impact of antibiotics (that promote CRE intestinal colonisation) on the faecal microbiota from healthy human donors. We demonstrated that antibiotics decreased the abundance of gut commensals (including *Bifidobacteriaceae* and *Bacteroidales*) in human faecal microbiota, resulting in an enrichment of nutrients and a depletion of microbial metabolites. The nutrient utilisation abilities, nutrient preferences, and metabolite inhibition susceptibilities of carbapenem-resistant *Escherichia coli*, *Klebsiella pneumoniae*, and *Enterobacter cloacae* strains were measured. Nutrients (which were elevated with antibiotics) acted as carbon and nitrogen sources to support CRE growth, where CRE

showed an ordered preference for specific nutrients. These nutrients were also increased in faeces from antibiotic-treated mice but decreased following intestinal colonisation with carbapenem-resistant *E. coli*. Microbial metabolites (which decreased with antibiotics) were inhibitory towards CRE growth *in vitro*. Carbapenem-resistant *E. coli* growth was decreased in faecal samples from mice treated with a mixture of inhibitory metabolites compared with PBS-treated mice. These findings demonstrate that killing gut commensals with antibiotics disrupts colonisation resistance by enriching nutrients that support CRE growth and depleting metabolites that inhibit CRE growth. These results support the development of new microbiome therapeutics to prevent CRE intestinal colonisation, which would also prevent the subsequent development of invasive CRE infections.

INTRODUCTION

Antibiotic resistance presents a serious threat to human health, resulting in treatment failures, infection relapses, longer hospitalisations, poor clinical outcomes, and increased healthcare costs[1]. Treatment options are increasingly limited, less effective, and may involve administration of antibiotics that are more toxic to the patient[2]. There is an urgent need to develop new treatments for infections by antibiotic-resistant bacteria. In particular, alternative approaches are required to prevent the development of invasive infections by extremely drug-resistant pathogens such as carbapenem-resistant *Enterobacteriaceae* (CRE), which present an urgent public health threat[2]. However, there are many difficulties associated with the development of new antibiotics to treat these multidrug-resistant infections[2].

The intestine is the primary colonisation site for CRE and serves as a reservoir of CRE that seed difficult-to-treat invasive infections (such as bloodstream infections and recurrent urinary tract infections)[3]. Therefore, one approach to prevent the development of invasive CRE infections would be to prevent CRE from colonising the intestine, or to decolonise patients with pre-existing CRE intestinal colonisation. However, to do so we must first understand what drives CRE colonisation in the intestines of susceptible patients.

118 Healthy gut microbiota exhibit colonisation resistance, where gut commensals prevent pathogens
119 from colonising the intestine. However, it is well established that broad spectrum antibiotics disrupt
120 colonisation resistance and significantly promote the expansion of pathogens within the intestine[4].
121 In particular, carbapenems, piperacillin/tazobactam, ciprofloxacin, and cephalosporins are known to
122 promote CRE intestinal colonisation[5]. The mechanisms of colonisation resistance that healthy gut
123 microbiota use to protect against CRE intestinal colonisation are not fully understood. However,
124 based on findings from other pathogens, nutrient competition and metabolite inhibition are expected
125 to play an important role[6-10].
126
127 Bacteria must have access to nutrients that support their growth to successfully colonise the
128 intestine. However, nutrients are limited within the intestine as bacteria with similar or "overlapping"
129 nutrient utilisation abilities will compete for these nutrients and occupy similar niches[11]. Different
130 bacteria have different nutrient utilisation abilities, and the diversity and concentration of the available
131 nutrients will impact their growth[12]. Although bacteria may be able to utilise a variety of nutrients,
132 they generally have a prioritised utilisation of nutrients that varies between different bacterial
133 species[13]. The nutrient-niche hypothesis predicts that antibiotic-mediated disruption of the gut
134 microbiota leads to reduced competition for nutrients and an increase in nutrient availability in the
135 gut, which could promote *Enterobacteriaceae* growth[14].
136
137 Nutrient metabolism by the gut microbiota results in the production of metabolites, some of which
138 may be inhibitory towards pathogen growth[7,8]. Polysaccharide fermentation results in the production
139 of metabolites such as short chain fatty acids (SCFAs; e.g. formate, acetate, propionate, butyrate,
140 valerate) and organic acids (e.g. succinate, lactate, ethanol)[15]. Protein fermentation results in the
141 production of SCFAs and branched chain fatty acids (BCFAs; e.g. isobutyrate and isovalerate)[15].
142 However, killing gut commensals with antibiotics can decrease the production of microbial
143 metabolites and enable pathogen growth[7,16].
144
145 Broad-spectrum antibiotics kill a wide range of gut commensals and promote the intestinal
146 colonisation with CRE[5]. However, to date previous studies have only identified a very small number

147 of nutrients or metabolites that are disrupted with antibiotics and involved in CRE intestinal
148 colonisation[16,17]. Given the severe impact of broad-spectrum antibiotics on the gut microbiota, we
149 expected that these antibiotics would have a much more significant impact on nutrient metabolism
150 in the intestine. Understanding how antibiotics disrupt colonisation resistance to promote CRE
151 growth will facilitate the rational design of microbiome therapeutics to prevent or treat CRE intestinal
152 colonisation, and therefore prevent the subsequent development of difficult-to-treat invasive CRE
153 infections. However, microbiome therapeutics that only deplete a small subset of the available
154 nutrients that CRE can utilise will have limited clinical impact to prevent or restrict CRE growth, as
155 CRE will switch nutrient metabolism to utilise alternative available nutrients.
156
157 We hypothesised that antibiotics significantly enrich for wide range and diversity of nutrients and
158 deplete a wide range and diversity of metabolites, resulting in a significant change in the nutrient and
159 metabolite landscape CRE encounter in antibiotic-treated gut microbiota and creating a niche that
160 promotes CRE growth. We demonstrated that broad-spectrum antibiotics that promote CRE growth
161 enriched for a wide range of nutrients in the intestine, generating a "nutrient-enriched niche" that
162 supports CRE growth. We also demonstrated that these broad-spectrum antibiotics also depleted a
163 wide range of metabolites and generated a “metabolite-depleted niche” that no longer inhibited CRE
164 growth. We showed that these nutrients could act as carbon and nitrogen sources to support CRE
165 growth, where CRE showed an ordered preference for specific nutrients. Oxygen availability is also
166 increased in an antibiotic-treated gut, and we showed that CRE growth was higher on these nutrients
167 in the presence of oxygen. Finally, we showed that microbial metabolites (that were decreased with
168 antibiotics) were inhibitory towards CRE growth. Together, these results demonstrated that killing
169 gut commensals with antibiotics reduces colonisation resistance by disrupting nutrient metabolism.
170 This results in an intestinal niche that supports the expansion of CRE by enriching nutrients that
171 support CRE growth and depleting metabolites that inhibit CRE growth. We demonstrated that
172 bacterial consortia that compose microbiome therapeutics must fully occupy the same nutrient-
173 defined intestinal niche that CRE occupy in the gut to effectively prevent or restrict CRE intestinal
174 growth.
175

176 **RESULTS**

177

178 ***Antibiotics decreased the abundance of important bacterial families in faecal microbiota***

179

180 We performed *ex vivo* faecal culture experiments to measure the effects of eight broad-spectrum
181 antibiotics on the faecal microbiota from 11 healthy human donors. Antibiotics tested included
182 meropenem (MEM), imipenem/cilastatin (IPM), ertapenem (ETP), piperacillin/tazobactam (TZP),
183 ciprofloxacin (CIP), ceftriaxone (CRO), ceftazidime (CAZ), and cefotaxime (CTX). These antibiotics
184 are frequently used clinically and known to promote the intestinal colonisation with CRE[5]. Faecal
185 cultures are highly reproducible, allowing for the parallel testing of multiple groups that are inoculated
186 from a single faecal sample[18]. For each experiment a faecal sample was inoculated into a distal gut
187 growth medium supplemented with one of the eight antibiotics or not supplemented with antibiotics
188 ("antibiotic-naïve" control). First, we measured how these different antibiotics (that promote
189 susceptibility to CRE intestinal colonisation) impacted the abundance of gut commensal taxa from
190 faecal microbiota.

191

192 We found that antibiotics decreased the absolute abundance of several bacterial families, in
193 particular *Bifidobacteriaceae* and families from the order *Bacteroidales* (**Fig. 1a**). Carbapenems
194 decreased the abundance of *Bifidobacteriaceae*, *Coriobacteriaceae*, *Bacteroidaceae*,
195 *Barnesiellaceae*, *Butyricicoccaceae,* and other bacterial families. TZP decreased the abundance of
196 *Bifidobacteriaceae* and *Bacteroidaceae*. CIP decreased the abundance of *Bifidobacteriaceae*,
197 *Barnesiellaceae* and *Sutterellaceae*. Cephalosporins decreased the abundance of
198 *Bifidobacteriaceae* only.

199

200 Overall, antibiotic treatment resulted in a decrease in the abundance of several bacterial families in
201 faecal microbiota, in particular *Bifidobacteriaceae* and families from the *Bacteroidales* order.

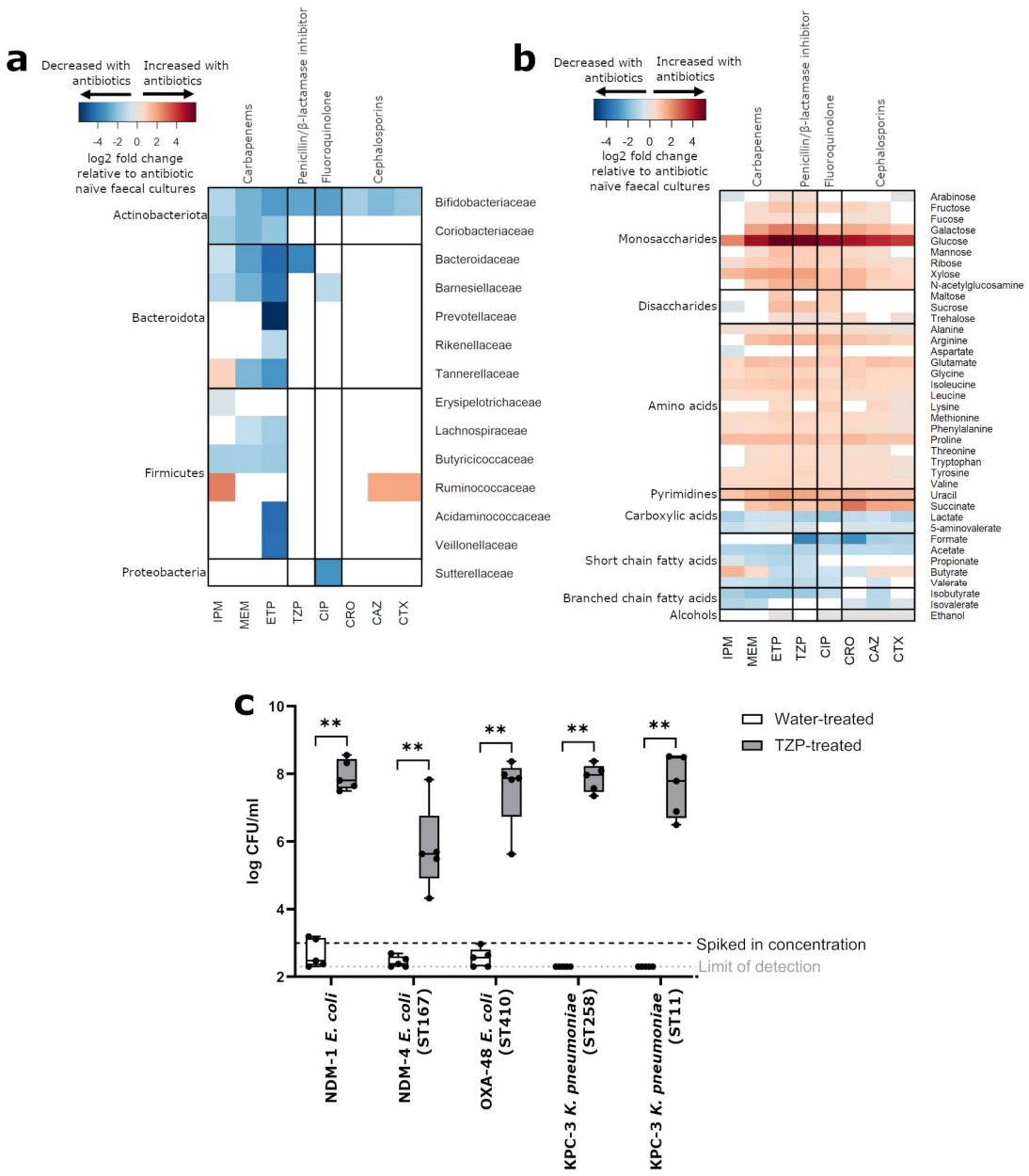

Figure 1: CRE growth is promoted in antibiotic-treated human faecal microbiota that had a significant decrease in the abundance of several bacterial families, a significant increase in the concentration of nutrients, and a significant decrease in the concentration of microbial metabolites. a) Log2 fold change in bacterial families significantly decreased with antibiotics (blue) or significantly increased with antibiotics (red), relative to antibiotic-naïve faecal cultures. Wilcoxon signed rank test of log-transformed abundances with Benjamini Hochberg false discovery rate (FDR) correction, $p<0.05$. Bacterial families, nutrients, and metabolites that were not significantly changed with antibiotics were not plotted (white). n = 11 healthy human faecal donors. **b)** Log2 fold change in nutrients and metabolites significantly increased with antibiotics (red) and nutrients and metabolites significantly decreased with antibiotics (blue), relative to antibiotic-naïve faecal cultures. Wilcoxon signed rank test with Benjamini Hochberg FDR, $p<0.05$. Bacterial families, nutrients, and metabolites that were not significantly changed with antibiotics were not plotted (white). n = 11 healthy human faecal donors. **c)** TZP treatment significantly promoted the growth of CRE in human faecal microbiota. Each CRE strain was spiked into TZP-treated or water-treated faecal cultures at a concentration of 10^3 CFU/ml at the start of the experiment (represented by the black horizontal dashed line). Limit of detection represented by the grey horizontal dotted line. n = 5 healthy human faecal donors, Mann-Whitney U test of log transformed CFU/ml, ** = $P \leq 0.01$.

203 ***Antibiotics enriched nutrients and depleted microbial metabolites in faecal microbiota***

204

205 Antibiotic-mediated killing of gut commensals can reduce competition for nutrients, resulting in an
206 increased availability of nutrients that could support pathogen growth. Antibiotics also decrease the
207 concentration of microbial metabolites which may be inhibitory to pathogen growth. However, we do
208 not know which nutrients and metabolites are impacted by treatment with different antibiotics that
209 promote the intestinal colonisation with CRE. Therefore, we also measured the effects of the different
210 antibiotics on nutrient availability and metabolite production in antibiotic-treated and antibiotic-naïve
211 faecal cultures using ^{1}H-NMR spectroscopy.

212

213 Antibiotic treatment of faecal microbiota increased the concentration of several nutrients, including
214 monosaccharides (in particular glucose), disaccharides, amino acids, uracil, and succinate (**Fig. 1b**).
215 Antibiotics also decreased the concentration of microbial metabolites, including SCFAs, BCFAs,
216 lactate, 5-aminovalerate, and ethanol (**Fig. 1b**). Butyrate decreased in ETP, TZP, CIP, and CRO-
217 treated faecal microbiota but increased in MEM, IPM, CAZ, and CTX-treated faecal microbiota.

218

219 Next, we spiked CRE isolates into antibiotic-treated and antibiotic-naïve faecal cultures to determine
220 whether the increase in nutrient availability and decrease in the concentration of microbial
221 metabolites led to environmental conditions that promoted CRE growth. We chose to test TZP in this
222 experiment because TZP has previously been demonstrated to promote the intestinal colonisation
223 of CRE in humans and mice.[5,19,20] Moreover, changes in bacterial families, nutrient availability, and
224 microbial metabolites in TZP-treated faecal microbiota were representative of changes in faecal
225 microbiota treated with the other antibiotics that were tested in this study (**Fig. 1a,b**). We
226 demonstrated that carbapenem-resistant *E. coli* and *K. pneumoniae* growth were significantly
227 promoted in TZP-treated faecal cultures and suppressed in antibiotic-naïve faecal cultures (**Fig. 1c**).

228

229 Overall, antibiotic treatment of a faecal microbiota resulted in an increase in monosaccharides,
230 disaccharides, amino acids, uracil, and succinate and a decrease in the concentration of SCFAs,
231 BCFAs, lactate, 5-aminovalerate, and ethanol. This created a nutrient-enriched niche that supported

232 CRE growth and a metabolite-depleted niche that no longer inhibited CRE growth.

233

234 ***Bacterial taxa that were decreased with antibiotics were positively correlated with microbial***

235 ***metabolites and negatively correlated with nutrients***

236

237 Regularised canonical correlation analysis (rCCA) is an unsupervised approach used to analyse the

238 correlation structure between two multivariate datasets that have been acquired from the same

239 samples[21]. We used rCCA modelling to measure correlations between 16S rRNA gene sequencing

240 data and ^{1}H-NMR spectroscopy data from antibiotic-treated and antibiotic-naïve faecal cultures. The

241 aim of this analysis was to link changes in bacterial families to changes in nutrients and metabolites

242 following antibiotic treatment, to provide targets for the future development of microbiome

243 therapeutics to restore colonisation resistance against CRE.

244

245 Unit representation plots show sample clustering projected into the XY-variate space (in this study,

246 X and Y represent the 16S rRNA sequencing dataset and ^{1}H-NMR spectroscopy dataset)[21]. The unit

247 representation plots showed a separation between antibiotic-treated and antibiotic-naïve faecal

248 cultures along the first canonical variate, indicating antibiotic treatment caused a separation in these

249 groups based on their bacterial taxa and nutrient/metabolite profiles (**Fig. S1**).

250

251 Correlation circle plots show the correlation structure between features and the canonical variates[21].

252 In these plots, features projected in the same direction from the origin have a positive correlation,

253 and features projected in opposite directions from the origin have a negative correlation. Features

254 sitting at farther distances from the origin have stronger correlations than features sitting closer to

255 the origin (features with weak correlations are not plotted). In this study, correlation circle plots

256 showed moderate and strong negative correlations between bacterial families that were decreased

257 with antibiotics and monosaccharides, disaccharides, amino acids, uracil, and succinate (**Fig. 2**).

258 They also showed moderate and strong positive correlations between bacterial families that were

259 decreased with antibiotics and SCFAs, BCFAs, 5-aminovalerate, and ethanol (**Fig. 2**).

260

261 Therefore, antibiotic treatment (using antibiotics that promote CRE intestinal colonisation) resulted
262 in a reduction of bacterial families that are positively correlated with metabolites (indicating that these
263 bacterial families may produce these metabolites) and negatively correlated with nutrients (indicating
264 that these bacterial families may consume these nutrients). This highlights the potential role of these
265 gut commensals for providing colonisation resistance against CRE in antibiotic-naïve faecal
266 microbiota.
267

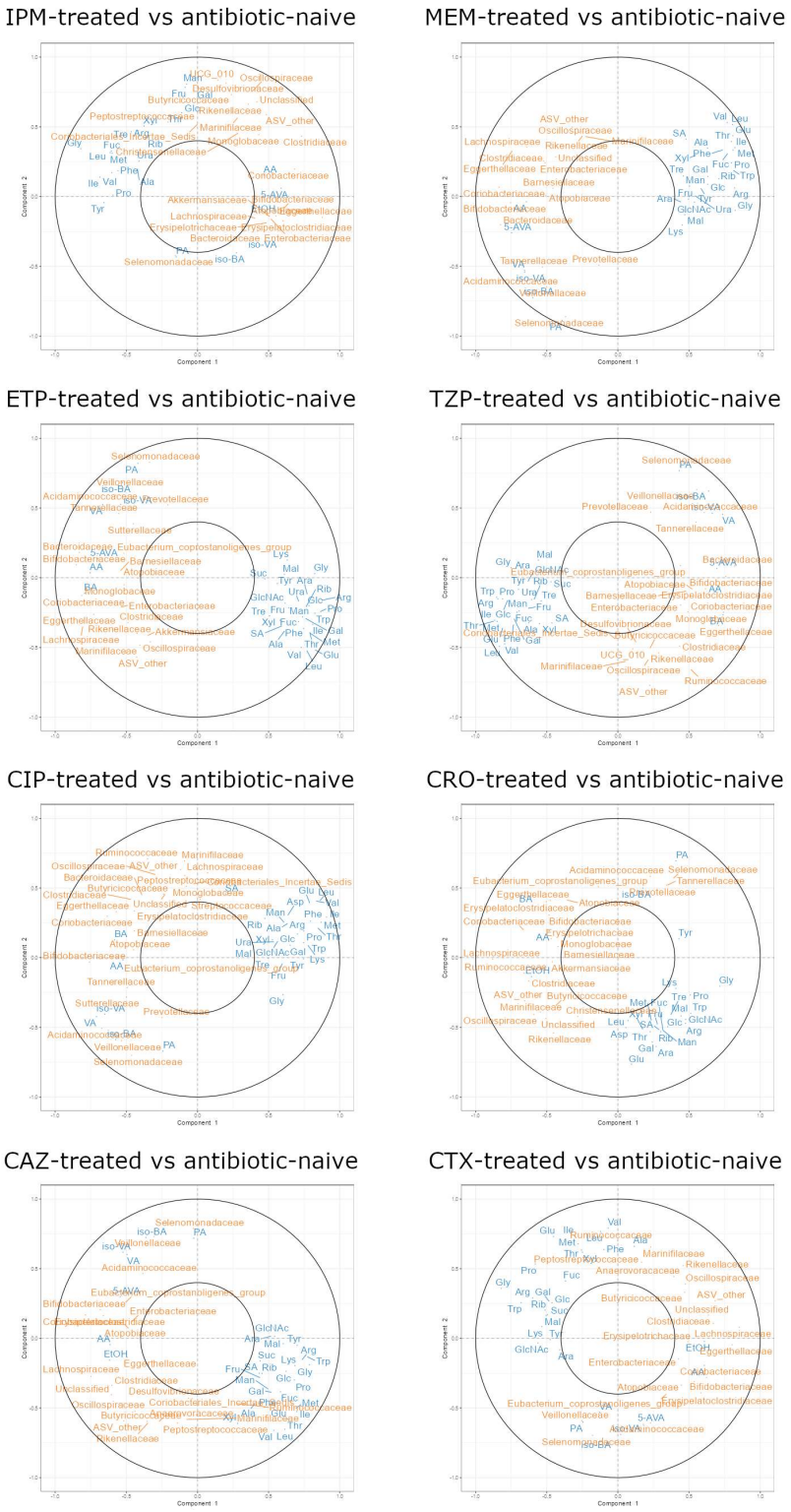

Figure 2. Bacterial families that were decreased in antibiotic-treated human faecal microbiota were positively correlated with microbial metabolites and negatively correlated with nutrients. rCCA model correlating 16S rRNA gene sequencing data (family level) and ^{1}H-NMR spectroscopy data (n = 11 healthy faecal donors). Correlation circle plot showing correlations between features from antibiotic-treated and antibiotic-naïve samples. Nutrients and metabolites are shown in blue and bacterial families are shown in orange. The following abbreviations are used for nutrients and metabolites: arabinose, Ara; fructose, Fru; fucose, Fuc; galactose, Gal; glucose, Glc; mannose, Man; ribose, Rib; xylose, Xyl; N-acetylglucosamine, GlcNAc; maltose, Mal; sucrose, Suc; trehalose, Tre; alanine, Ala; arginine, Arg; aspartate, Asp; glutamate, Glu; glycine, Gly; isoleucine, Ile; leucine, Leu; lysine, Lys; methionine, Met; phenylalanine, Phe; proline, Pro; threonine, Thr; tryptophan, Trp; tyrosine, Tyr; valine, Val; uracil, Ura; succinate, SA; lactate, LA; 5-aminovalerate, 5-AVA; formate, FA; acetate, AA; propionate, PA; butyrate, BA; valerate, VA; isobutyrate, iso-BA; isovalerate, iso-VA; ethanol, EtOH.

268

269 ***CRE can grow using nutrients that were elevated in antibiotic-treated faecal microbiota***

270

271 We demonstrated that monosaccharides, disaccharides, amino acids, uracil, and succinate were
272 elevated with antibiotic treatment of faecal microbiota (**Fig. 1b**). Our next aim was to demonstrate
273 that these nutrients could support CRE growth. The growth of carbapenem-resistant *Escherichia coli*
274 (NDM-1), *Klebsiella pneumoniae* (NDM-1), and *Enterobacter cloacae* (NDM-1) were measured in a
275 mixture of these nutrients supplemented into M9 minimal medium (lacking any other carbon or
276 nitrogen sources) and changes in OD_{600} were measured over time. Antibiotic-mediated disruption of
277 the gut microbiota significantly increases oxygen availability in the gut, which may allow
278 *Enterobacteriaceae* to grow better on available carbon sources[14]. Therefore, we investigated CRE
279 growth in both the presence and absence of oxygen.

280

281 We showed that CRE growth was supported by the nutrient mixture, where these nutrients were
282 acting as the sole carbon and nitrogen sources (**Fig. 3**). For each CRE isolate growth was
283 significantly higher under aerobic conditions compared to anaerobic conditions.

284

285 Therefore, CRE can grow on nutrients that were elevated with antibiotics, and increased oxygen
286 availability promotes higher levels of CRE growth on these nutrients. This led us to conclude that the
287 significant increase of these nutrients following antibiotics contributes to the loss of colonisation
288 resistance against CRE.

289

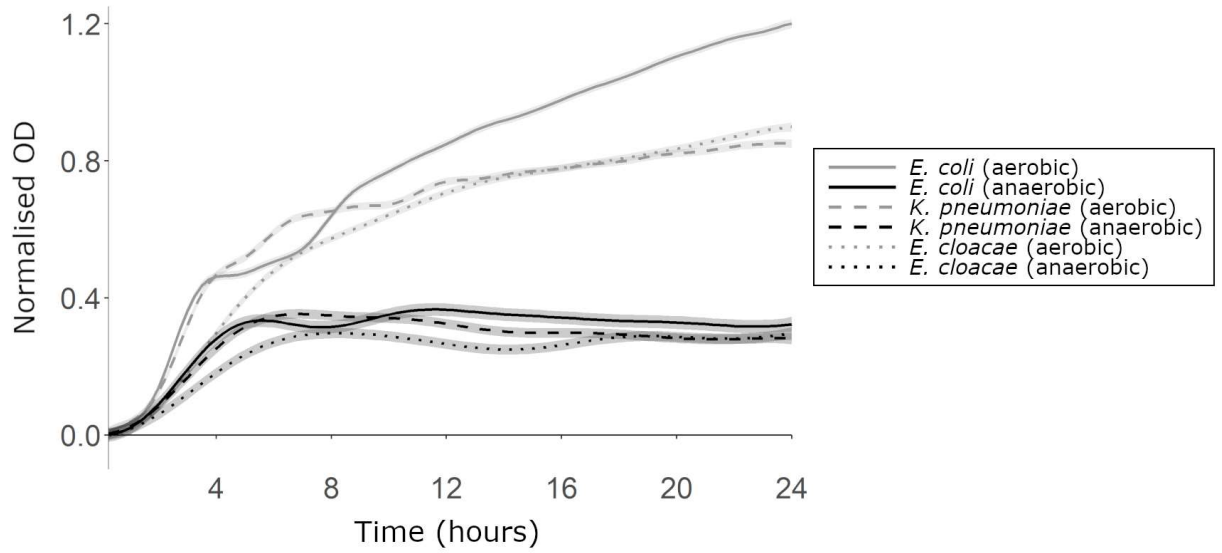

Figure 3: CRE growth was supported by a mixture of nutrients that were elevated in antibiotic-treated faecal microbiota. AMiGA-predicted growth curves for NDM-1 *E. coli*, NDM-1 *K. pneumoniae*, and NDM-1 *E. cloacae* grown on M9 minimal medium supplemented with a mixture of nutrients under anaerobic or aerobic conditions. Growth of each isolate was measured with 6 replicates in 2 independent experiments. The predicted mean of growth is shown with bold lines and the predicted 95% credible intervals are shown with the shaded bands.

CRE can use monosaccharides, disaccharides, and amino acids as carbon sources to support their growth

Above we demonstrated that a mixture of monosaccharides, disaccharides, amino acids, uracil, and succinate were able to support CRE growth in a minimal medium (**Fig. 3**). However, it was not clear which specific nutrients were utilised by each CRE isolate. Therefore, we next tested which individual nutrients could act as sole carbon sources to support CRE growth. The carbon utilisation abilities of *E. coli* (NDM-1), *K. pneumoniae* (NDM-1), and *E. cloacae* (NDM-1) were demonstrated by adding a single carbon source into M9 minimal medium and monitoring changes in OD_{600} over time.

When grown anaerobically, *E. coli*, *K. pneumoniae*, and *E. cloacae* could use most monosaccharides and disaccharides as carbon sources to support their growth (**Fig. 4**), with some carbon sources supporting higher levels of growth than others (**Fig. S2**). *E. coli* could grow on arabinose, fructose, galactose, glucose, mannose, xylose, N-acetylglucosamine, and trehalose. *K. pneumoniae* could grow on arabinose, fructose, galactose, glucose, mannose, xylose, N-acetylglucosamine, maltose, sucrose, and trehalose. *E. cloacae* could grow on arabinose, fructose, galactose, glucose, mannose,

307 ribose, xylose, N-acetylglucosamine, maltose, sucrose, and trehalose. Carbon sources that did not
308 support *E. coli*, *K. pneumoniae*, and *E. cloacae* growth under anaerobic conditions are shown in **Fig.**
309 **S3**.
310
311 When grown aerobically, *E. coli*, *K. pneumoniae*, and *E. cloacae* could use the same carbon sources
312 that were used anaerobically plus additional carbon sources to support their growth (**Fig. 4**). Again,
313 some carbon sources supported higher levels of growth than others (**Fig. S2**). *E. coli* could grow on
314 arabinose, fructose, galactose, glucose, mannose, ribose, xylose, N-acetylglucosamine, maltose,
315 sucrose, trehalose, and alanine. *K. pneumoniae* could grow on arabinose, fructose, galactose,
316 glucose, mannose, ribose, xylose, N-acetylglucosamine, maltose, sucrose, trehalose, alanine,
317 glutamate, and proline. *E. cloacae* could grow on arabinose, fructose, fucose, galactose, glucose,
318 mannose, ribose, xylose, N-acetylglucosamine, maltose, sucrose, trehalose, alanine, and glutamate.
319 Carbon sources that did not support *E. coli*, *K. pneumoniae*, and *E. cloacae* growth under aerobic
320 conditions are shown in **Fig. S3**.
321
322
323 Overall, *E. coli*, *K. pneumoniae*, and *E. cloacae* were able to utilise individual nutrients as carbon
324 sources to support their growth. However, each isolate was able to grow to higher levels when grown
325 aerobically versus anaerobically. Moreover, each isolate was also able to grow on a larger number
326 of carbon sources aerobically versus anaerobically.

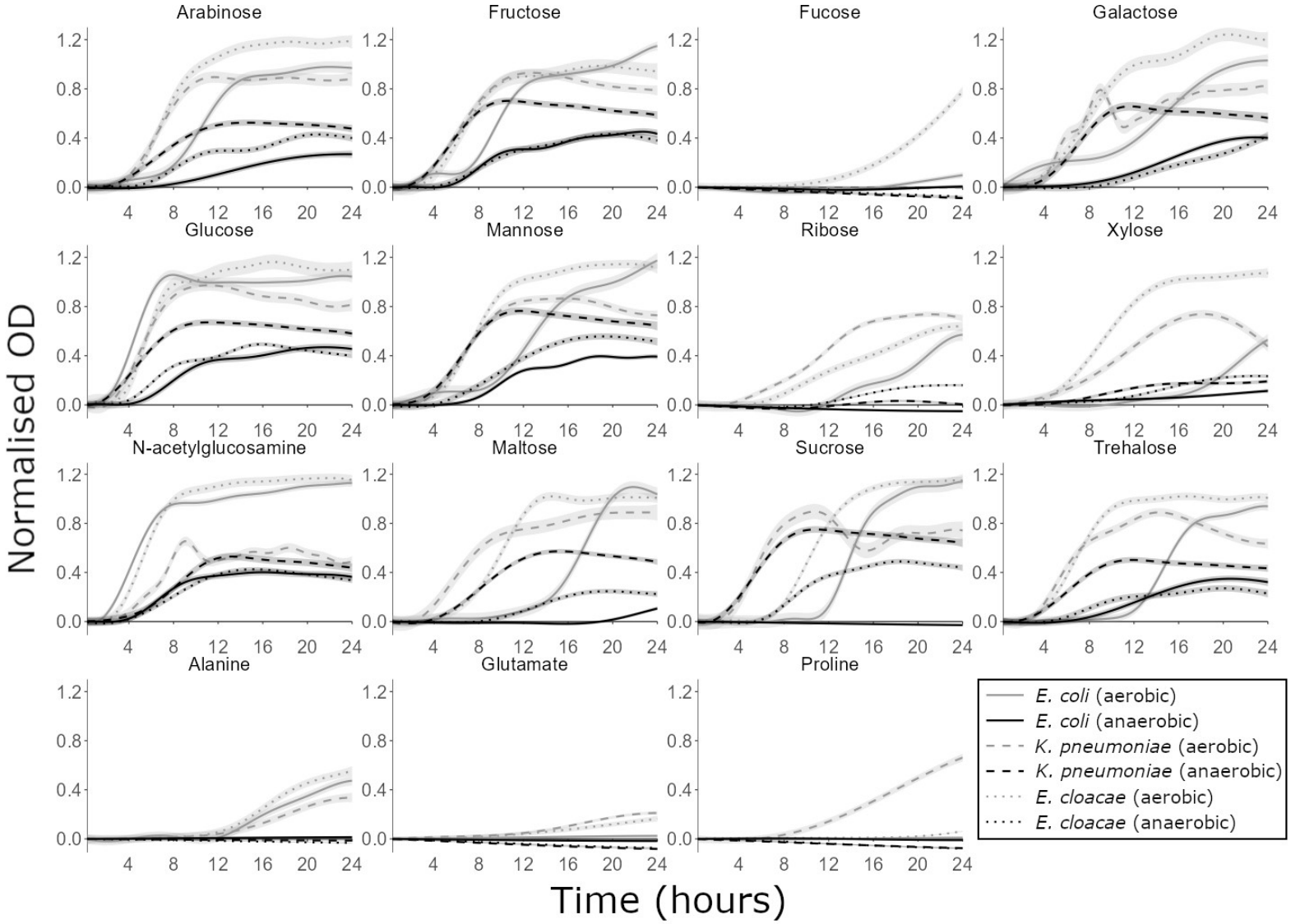

Figure 4: CRE growth was supported by many individual carbon sources that were elevated in antibiotic-treated faecal microbiota. AMiGA-predicted growth curves for NDM-1 *E. coli*, NDM-1 *K. pneumoniae*, and NDM-1 *E. cloacae* grown on M9 minimal medium supplemented with a single carbon source (or water as the no carbon control) under anaerobic or aerobic conditions. Growth of each isolate was measured with 6 replicates in 2-3 independent experiments. The predicted mean of growth is shown with bold lines and the predicted 95% credible intervals are shown with the shaded bands.

327

328 ***CRE can use amino acids, N-acetylglucosamine, and uracil as nitrogen sources to support***
329 ***their growth***
330
331 Above we showed that most amino acids and uracil were not used as carbon sources by CRE.
332 However, amino acids, N-acetylglucosamine, and uracil may instead act as nitrogen sources to
333 support CRE growth. Therefore, we next tested the nitrogen utilisation abilities of *E. coli* (NDM-1),
334 *K. pneumoniae* (NDM-1), and *E. cloacae* (NDM-1) by adding a single nitrogen source into M9
335 minimal medium and monitoring changes in OD_{600} over time.
336
337 When grown anaerobically, *E. coli*, *K. pneumoniae*, and *E. cloacae* could use some amino acids and
338 N-acetylglucosamine as nitrogen sources to support their growth (**Fig. 5**), with some nitrogen
339 sources supporting higher levels of growth than others (**Fig. S4**). *E. coli* could grow on arginine,
340 aspartate, valine, and N-acetylglucosamine. *K. pneumoniae* and *E. cloacae* could grow on arginine,
341 aspartate, and N-acetylglucosamine.
342
343 When grown aerobically, *E. coli*, *K. pneumoniae*, and *E. cloacae* could use the same nitrogen
344 sources that were used anaerobically plus additional nitrogen sources to support their growth (**Fig.**
345 **5**). Again, some nitrogen sources supported higher levels of growth than others (**Fig. S4**). *E. coli*
346 could grow on alanine, arginine, aspartate, glutamate, glycine, isoleucine, leucine, lysine,
347 methionine, proline, threonine, tryptophan, tyrosine, valine, N-acetylglucosamine, and uracil. *K.*
348 *pneumoniae* could grow on alanine, arginine, aspartate, glutamate, glycine, isoleucine, leucine,
349 lysine, methionine, proline, and uracil. *E. cloacae* could grow on alanine, arginine, aspartate,
350 glutamate, glycine, isoleucine, leucine, lysine, methionine, phenylalanine, proline, threonine, N-
351 acetylglucosamine, and uracil.
352
353 Overall, *E. coli*, *K. pneumoniae*, and *E. cloacae* were able to utilise individual nutrients as nitrogen
354 sources to support their growth. Each isolate was able to grow to higher levels when grown
355 aerobically versus anaerobically. Moreover, each isolate was also able to grow on a larger number
356 of nitrogen sources aerobically versus anaerobically.

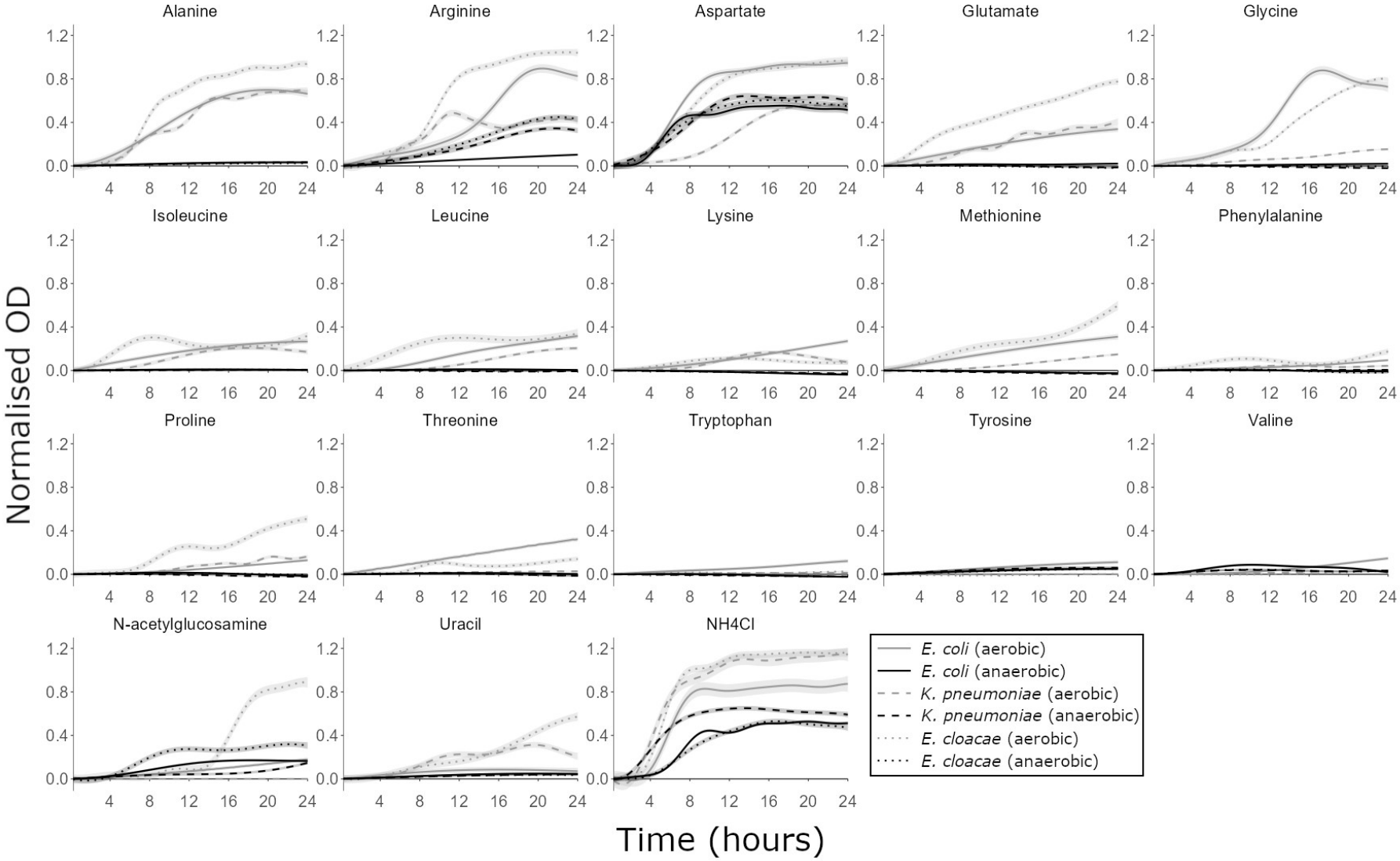

Figure 5: CRE growth was supported by individual nitrogen sources that were elevated in antibiotic-treated faecal microbiota. AMiGA-predicted growth curves for NDM-1 *E. coli*, NDM-1 *K. pneumoniae*, and NDM-1 *E. cloacae* grown on M9 minimal medium supplemented with a single nitrogen source (or water as the no nitrogen control) under anaerobic or aerobic conditions. Growth of each isolate was measured with 6 replicates in 2-3 independent experiments. The predicted mean of growth is shown with bold lines and the predicted 95% credible intervals are shown with the shaded bands. NH_4Cl was used as a positive control for growth as a sole nitrogen source.

358 ***CRE had an ordered preference of nutrients when provided with a mixture of nutrients***

359

360 Above we demonstrated that CRE can use monosaccharides, disaccharides, and some amino acids
361 as carbon sources and amino acids, N-acetylglucosamine, and uracil as nitrogen sources to support
362 their growth. However, carbon utilisation assays were carried out using a single nitrogen source and
363 nitrogen utilisation assays were carried out using a single carbon source. As we demonstrated in
364 **Fig. 1b**, there are several carbon and nitrogen sources that are available to support CRE growth
365 following antibiotic treatment, and it is not clear whether CRE have preferences for some carbon or
366 nitrogen sources over others. It is also not clear whether the presence of some carbon or nitrogen
367 sources will influence the utilisation of other carbon or nitrogen sources, as has been previously
368 demonstrated for commensal *E. coli*[22]. Therefore, the nutrient utilisation abilities of *E. coli* (NDM-1),
369 *K. pneumoniae* (NDM-1), and *E. cloacae* (NDM-1) were measured by adding a mixture of these
370 nutrients into M9 minimal medium (lacking any other carbon or nitrogen sources) and monitoring
371 changes in nutrient concentration over time by ^{1}H-NMR spectroscopy.

372

373 *E. coli*, *K. pneumoniae*, and *E. cloacae* were able to utilise nearly all the monosaccharides and
374 disaccharides tested (**Fig. 6**). When grown anaerobically, *E. coli* and *E. cloacae* had high utilisation
375 levels of all monosaccharides and disaccharides. *K. pneumoniae* had high utilisation of all
376 monosaccharides and disaccharides except for fucose, which was not utilised. When grown
377 aerobically, *E. coli* had high utilisation of all monosaccharides and disaccharides except for sucrose,
378 which had moderate utilisation. *K. pneumoniae* had high utilisation of all monosaccharides and
379 disaccharides except for fucose, which was not utilised. *E. cloacae* had high utilisation of all
380 monosaccharides and disaccharides.

381

382 *E. coli*, *K. pneumoniae*, and *E. cloacae* showed variable amino acid utilisation patterns. Under
383 anaerobic conditions, *E. coli* had high utilisation of aspartate and lysine, moderate utilisation of
384 tryptophan, and low utilisation of the other amino acids (except for alanine or proline, which were not
385 utilised). *K. pneumoniae* had high utilisation of aspartate and lysine, and low utilisation of the other
386 amino acids (except for alanine, proline, and tryptophan, which were not utilised). *E. cloacae* had

387 high utilisation of aspartate, threonine, and arginine, and low utilisation of the other amino acids
388 (except for alanine, proline, tryptophan, and tyrosine, which were not utilised). Under aerobic
389 conditions, *E. coli* had high utilisation of aspartate and tryptophan, moderate utilisation of glutamate,
390 lysine, and threonine, and low utilisation of the other amino acids (except for proline, which was not
391 utilised). *K. pneumoniae* had high utilisation of aspartate, lysine, and threonine, moderate utilisation
392 of glutamate, and low utilisation of the other amino acids (except for tryptophan, which was not
393 utilised). *E. cloacae* had high utilisation of aspartate, threonine, and arginine, moderate utilisation of
394 glutamate, and low utilisation of the other amino acids (except for proline, tryptophan, and tyrosine,
395 which were not utilised). *E. cloacae* produced low levels of lysine both anaerobically and aerobically.
396
397 Uracil utilisation also varied by isolate under anaerobic and aerobic conditions. *E. coli* had moderate
398 utilisation of uracil under anaerobic and aerobic conditions. *K. pneumoniae* did not use uracil under
399 anaerobic conditions but utilised uracil at low levels under aerobic conditions. *E. cloacae* did not use
400 uracil under anaerobic and aerobic conditions.
401
402 The rate at which nutrients were utilised was different for *E. coli*, *K. pneumoniae*, and *E. cloacae*
403 (**Fig. S5**). Some nutrients were used more quickly than others, indicating that each CRE isolate had
404 its own ordered preference of nutrients. Moreover, aerobically incubated CRE cultures utilised most
405 nutrients more rapidly than anaerobically incubated CRE cultures.
406
407 Succinate was produced by all CRE isolates under both anaerobic and aerobic conditions. Other
408 metabolites produced by the CRE isolates included acetate, ethanol, and formate (**Fig. S6**).
409
410 In summary, these results led us to conclude that *E. coli*, *K. pneumoniae*, and *E. cloacae* had an
411 ordered preference for nutrients and that nutrient utilisation was different in the presence and
412 absence of oxygen.

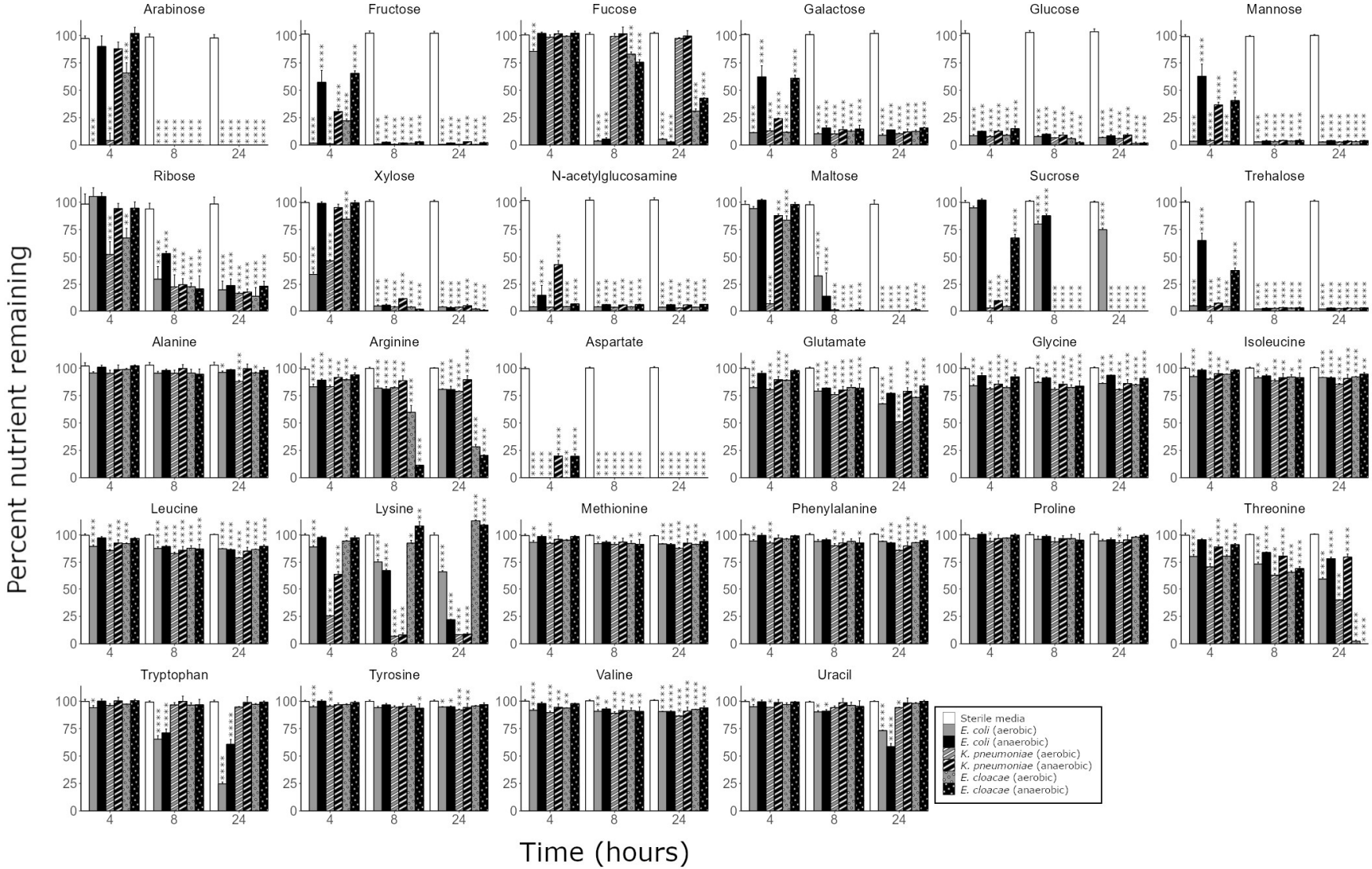

Figure 6: CRE isolates had an ordered preference of nutrients when cultured in a mixture of nutrients that were elevated in antibiotic-treated faecal microbiota. Percent of nutrients remaining in M9 minimal medium supplemented with a mixture of nutrients, inoculated with NDM-1 *E. coli*, NDM-1 *K. pneumoniae*, or NDM-1 *E. cloacae*, and incubated under anaerobic or aerobic conditions. Nutrient concentrations were measured by ^{1}H-NMR spectroscopy. Two-way mixed ANOVA followed by pairwise comparisons with Bonferroni correction. * = P ≤ 0.05, ** = P ≤ 0.01, *** = P ≤ 0.001, **** = P ≤ 0.0001, n=3 replicates for each CRE isolate and n=4 replicates for the sterile media controls.

414 ***Carbapenem-resistant* E. coli *utilised nutrients that were elevated in the faecal microbiota***
415 ***from TZP-treated mice***
416
417 Next, we used a mouse model of carbapenem-resistant *E. coli* intestinal colonisation to measure
418 changes in nutrient availability in mouse faeces following TZP treatment and NDM-1 *E. coli*
419 colonisation. Mice were administered TZP or saline for 5 days, and NDM-1 *E. coli* was orally
420 administered to the mice on the third day of TZP/saline administration (**Fig. 7a**). TZP-treated mice
421 had significantly higher *E. coli* counts in their faeces compared to saline-treated mice, demonstrating
422 that antibiotics disrupted colonisation resistance against carbapenem-resistant *E. coli* (**Fig. 7b**).
423
424 Faecal samples were collected from mice before TZP administration, after TZP administration but
425 before *E. coli* administration, and after TZP and *E. coli* administration. Changes in nutrients and
426 metabolites were measured by ^{1}H-NMR spectroscopy. The faeces of TZP-treated mice had
427 significantly increased concentrations of nutrients compared to faeces collected prior to TZP
428 treatment, including increases in monosaccharides (arabinose, fructose, galactose, glucose, xylose,
429 N-acetylglucosamine), disaccharides (sucrose, trehalose), and amino acids (arginine, aspartate,
430 glutamate, isoleucine, leucine, lysine, phenylalanine, proline, threonine, tryptophan, tyrosine, valine)
431 (**Fig. 7c**, heatmap on the left). TZP treatment also decreased the concentration of microbial
432 metabolites, including acetate, propionate, isobutyrate, ethanol, and lactate. Following colonisation
433 with NDM-1 *E. coli* there was a significant decrease in nutrients that we demonstrated can be utilised
434 by *E. coli* to support its growth, including monosaccharides (arabinose, fructose, galactose, glucose,
435 xylose, N-acetylglucosamine), disaccharides (sucrose, trehalose), amino acids (alanine, arginine,
436 aspartate, glutamate, lysine, tryptophan, tyrosine), and uracil (**Fig. 7c**, heatmap on the right).
437
438 Overall, antibiotic treatment of faecal microbiota from mice resulted in an increase in the
439 concentration of nutrients and a decrease in the concentration of microbial metabolites, supporting
440 observations from our *ex vivo* human faecal culture experiments (**Fig. 1**). Colonisation of the mouse
441 intestine with NDM-1 *E. coli* resulted in a decrease in nutrients that we demonstrated can be utilised
442 by *E. coli in vitro* (**Figs. 4, 5, 6**), supporting our hypothesis that *E. coli* consumes these nutrients to

443 support its growth.

444

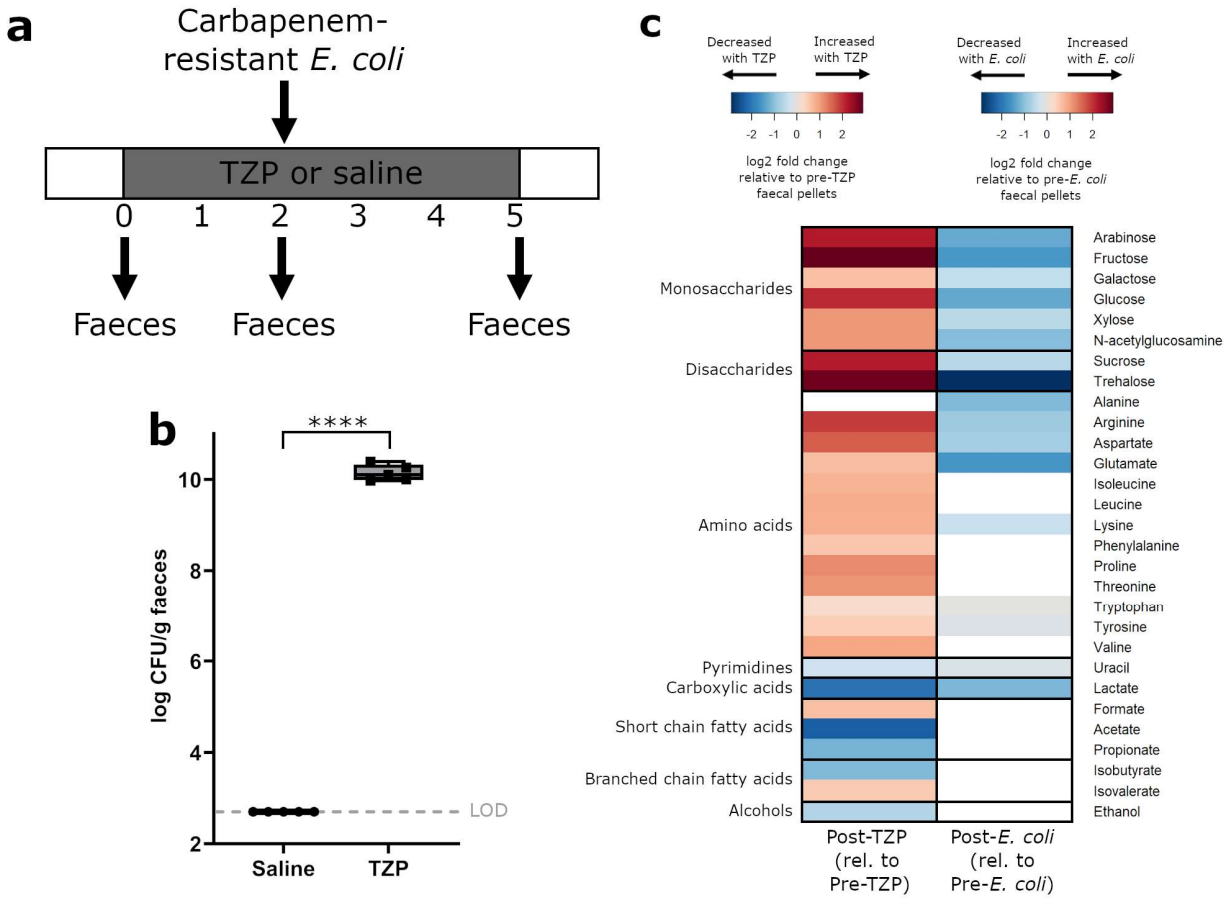

Figure 7: Nutrients that were elevated with TZP treatment decreased with *E. coli* colonisation in faeces from a mouse model of intestinal CRE colonisation. a) Experimental design. Mice were administered TZP or saline for 5 days and were fed by oral gavage with NDM-1 *E. coli* on the third day of TZP/saline administration. Faeces were collected before TZP administration, after TZP administration but before *E. coli* administration, and after TZP and *E. coli* administration. **b)** NDM-1 *E. coli* counts from mouse faecal pellets following *E. coli* administration (at the end of the TZP dosing period). The box excludes the upper and lower 25% (quartiles) of data, and the lines go to maximum and minimum values. Unpaired t-test of log10-transformed counts. n=5 mice per group, **** = P ≤ 0.0001. **c)** Log2 fold change in nutrients and metabolites significantly changed with interventions. For comparison of post-TZP treated faeces relative to pre-TZP treated faeces (heatmap on the left), nutrients and metabolites that were significantly increased with TZP are shown in red, and nutrients and metabolites that were significantly decreased with TZP are shown in blue (n=9 mice per group). For comparison of TZP-treated faeces post-*E. coli* colonisation relative to TZP-treated faeces pre-*E. coli* colonisation (heatmap on the right), nutrients and metabolites that were significantly decreased with *E. coli* colonisation are shown in blue (n=4 mice per group). Paired t-test with Benjamini Hochberg FDR, p<0.05. Nutrients and metabolites that were not significantly different were not plotted (white). LOD = limit of detection.

445

446 ***CRE growth was inhibited by microbial metabolites that were depleted in antibiotic-treated***

447 ***faecal microbiota***

448

449 Microbial metabolites have previously been demonstrated to inhibit the growth of intestinal

450 pathogens[7,16]. Nutrients are metabolised to produce metabolites, and therefore increased nutrient
451 availability is linked to reduced metabolite production. We demonstrated that microbial metabolites
452 were decreased in antibiotic-treated faecal microbiota (**Fig. 1b**). Therefore, we next tested whether
453 microbial metabolites (that were decreased with antibiotics) were capable of inhibiting CRE growth.
454
455 First, we measured the concentration of microbial metabolites in faeces from 12 healthy human
456 donors to determine the concentration of these metabolites in antibiotic-naïve faecal microbiota
457 (**Table S1**). We used these measurements to define a minimum, average, and maximum
458 concentration to test in the metabolite inhibition assays.
459
460 First, we tested whether a mixture of metabolites that were decreased with antibiotics (formate,
461 acetate, propionate, butyrate, valerate, isobutyrate, isovalerate, lactate, 5-aminovalerate, and
462 ethanol) could directly inhibit CRE growth in an inhibition assay. LB was supplemented with the
463 metabolite mixture, where each metabolite was added to mimic the average concentration that was
464 measured in healthy human faeces. As pH has been demonstrated to influence the ability of SCFAs
465 to inhibit pathogen growth, the metabolite mixture was tested at three pH conditions mimicking the
466 pH found in the healthy large intestine: 6, 6.5, and 7[16,23]. We showed that the metabolite mixture
467 inhibited the growth of *E. coli*, *K. pneumoniae*, and *E. cloacae* at pH 6, 6.5, and 7 (**Fig. 8a**). However,
468 inhibition was higher at pH 6 and 6.5 compared to pH 7.
469
470 Next, we measured CRE growth in the presence of each individual metabolite at three different
471 concentrations: the minimum, average, and maximum concentrations measured in healthy faeces.
472 These experiments were performed at pH 6.5 as this pH was representative of the large intestine
473 and showed strong inhibition in the mixed metabolite experiment (as shown in **Fig. 8a**). *E. coli* was
474 inhibited by acetate at low, average, and high concentrations, by propionate, valerate, and ethanol
475 at average and high concentrations, and by butyrate at high concentrations (**Fig. 8b**). *K. pneumoniae*
476 was inhibited by butyrate at low, average, and high concentrations, and by acetate, propionate,
477 valerate, isobutyrate, and isovalerate at average and high concentrations (**Fig. 8c**). *E. cloacae* was
478 inhibited by butyrate and valerate at low, average, and high concentrations, by acetate, propionate,

479 isobutyrate, and isovalerate at average and high concentrations, and by ethanol at the high
480 concentration (**Fig. 8d**).
481
482 In summary, we demonstrated that specific microbial metabolites (that were decreased following
483 antibiotic treatment of faecal microbiota) were inhibitory towards CRE isolates. This led us to
484 conclude that the significant decrease of these metabolites following antibiotics contributes to the
485 loss of colonisation resistance against CRE.

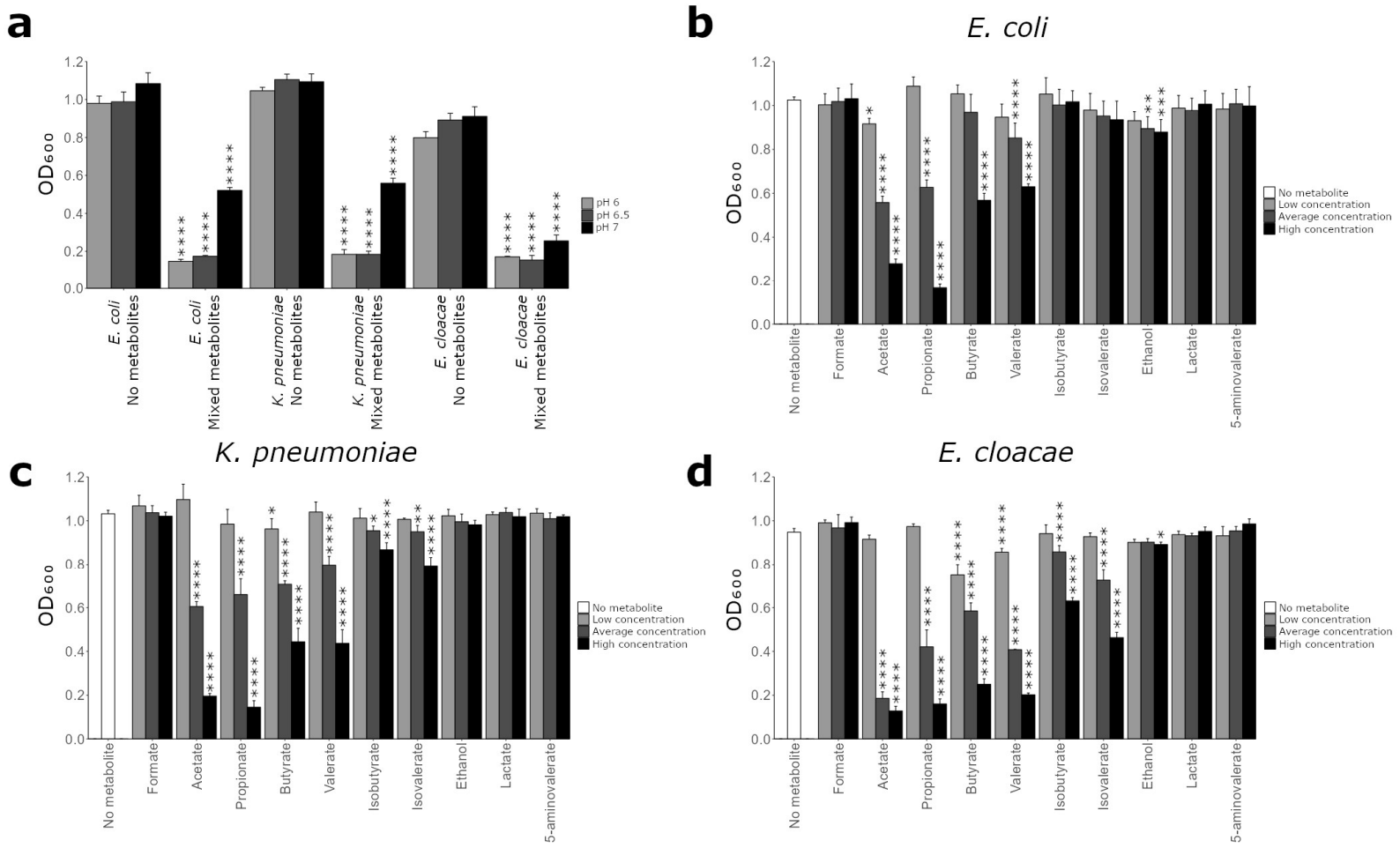

Figure 8: CRE growth was inhibited by microbial metabolites that were decreased in antibiotic-treated faecal microbiota. a) CRE growth was inhibited by a mixture of metabolites that were decreased in antibiotic-treated faecal microbiota. NDM-1 *E. coli*, NDM-1 *K. pneumoniae*, or NDM-1 *E. cloacae* were grown in LB supplemented with a metabolite mixture (mimicking average human faecal concentrations) or unsupplemented ("no metabolite" control) at pH 6, 6.5, or 7. Growth of each isolate was measured with 6 replicates in 2 independent experiments. Unpaired t-test comparing metabolite mixture to the no metabolite control at the corresponding pH. **b-d**) CRE growth was inhibited by individual metabolites in a dose-dependent manner. Growth of NDM-1 *E. coli*, NDM-1 *K. pneumoniae*, or NDM-1 *E. cloacae* in LB supplemented with an individual metabolite at low, average, or high concentrations (mimicking human faecal concentrations) or unsupplemented ("no metabolite" control) at pH 6.5. Growth of each isolate was measured with 6 replicates in 2 independent experiments. One-way ANOVA followed by Dunn's multiple comparison test (each metabolite was compared to the no metabolite control). * = P ≤ 0.05, ** = P ≤ 0.01, *** = P ≤ 0.001, **** = P ≤ 0.0001.

487 ***Carbapenem-resistant* E. coli *growth was inhibited by a mixture of microbial metabolites in a***
488 ***mouse model of CRE intestinal colonisation***
489
490 Next, we administered a mixture of inhibitory metabolites as an intervention in a mouse model of
491 intestinal CRE colonisation to determine whether these metabolites could inhibit the growth of NDM-
492 1 *E. coli in vivo*. TZP-treated mice colonised with NDM-1 *E. coli* were administered a mixture of
493 metabolites (acetate, propionate, butyrate, and valerate) or PBS (as a vehicle control; **Fig. 9a**). We
494 chose to test these metabolites in mice as they were inhibitory against all three CRE isolates when
495 tested individually (**Fig. 8**) and when tested together as a mixture (**Fig. S7**). Each metabolite was
496 administered to the mice in their triglyceride form (i.e. as a mixture of glycerol triacetate, glycerol
497 tripropionate, glycerol tributyrate, and glycerol trivalerate) to avoid rapid absorption of SCFAs
498 following oral gavage and to obtain sufficient concentrations of these SCFAs in the gastrointestinal
499 tract[7]. The triglyceride forms of these SCFAs are hydrolysed by lipases to release acetate,
500 propionate, butyrate, and valerate, respectively, in the intestine[24].
501
502 Prior to the administration of the metabolite mixture or PBS to mice, there was no significant
503 difference in NDM-1 *E. coli* counts in the faeces from each group ($p>0.9999$). However, there was a
504 significant decrease in NDM-1 *E. coli* counts in the faeces of metabolite-treated mice compared to
505 PBS-treated mice (**Fig. 9b**, $p=0.0397$). After 3 doses of the metabolite mixture or PBS, metabolite-
506 treated mice had an average of 87% less *E. coli* CFU per gram of faeces compared to PBS-treated
507 mice.
508
509 Overall, we demonstrated that metabolites that were decreased in antibiotic-treated human faecal
510 microbiota (acetate, propionate, butyrate, and valerate) were able to inhibit NDM-1 *E. coli* in a mouse
511 model of intestinal CRE colonisation, highlighting their important role in providing colonisation
512 resistance against CRE.
513

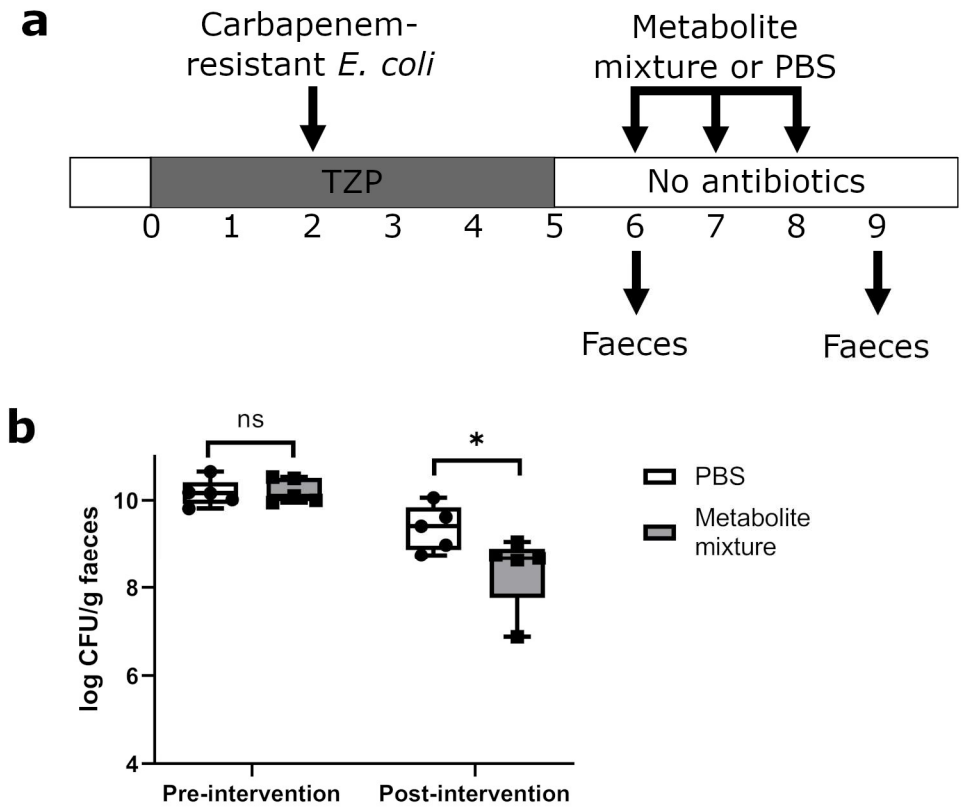

Figure 9: Microbial metabolites significantly decreased carbapenem-resistant *E. coli* growth in faeces from a mouse model of intestinal CRE colonisation. a) Experimental design. Mice were administered TZP for 5 days and were orally administered NDM-1 *E. coli* on the third day of TZP administration. Mice were then fed by oral gavage with a mixture of metabolites (glycerol triacetate, glycerol tripropionate, glycerol tributyrate, and glycerol trivalerate) or PBS for 3 days. **b)** NDM-1 *E. coli* counts were quantified from mouse faecal pellets just before metabolite mixture or PBS administration (pre-intervention) and at the end of metabolite mixture or PBS administration (post-intervention). The box excludes the upper and lower 25% (quartiles) of data, and the lines go to maximum and minimum values. Mann-Whitney U test of log10-transformed counts. n=5 mice per group, * = P ≤ 0.05.

DISCUSSION

In this study we demonstrated that antibiotic-mediated disruption of the gut microbiota (using antibiotics that promote CRE intestinal colonisation) led to the development of a nutrient-enriched and metabolite-depleted niche that was favourable for CRE growth. We showed that CRE can use these elevated nutrients as carbon and nitrogen sources to support their growth, where CRE show an order of preference for specific nutrients. CRE growth was higher on these nutrients in an oxygenated environment, which has been associated with antibiotic treatment. We also showed that specific microbial metabolites that were decreased with antibiotics were able to inhibit CRE growth.

525 We showed that healthy faecal microbiota treated with antibiotics that promote CRE intestinal
526 colonisation resulted in a decrease of several bacterial families, in particular *Bifidobacteriaceae*
527 (decreased with all antibiotics tested), families belonging to *Bacteroidales* (decreased with
528 carbapenems, TZP, and CIP), and *Coriobacteriaceae* (decreased with carbapenems). Our results
529 are supported by previous studies in healthy humans which also demonstrated a decrease in
530 *Bifidobacterium* and *Bacteroides* with these antibiotics[25-30]. Our results are also supported by a
531 recent study which demonstrated that CRE-positive patients had lower amounts of *Bacteroides*
532 *dorei*, *Bifidobacterium bifidum*, *Bifidobacterium pseudocatenulatum*, and *Collinsella aerofaciens* in
533 their faeces compared to CRE-negative patients[31]. Moreover, a recent study demonstrated that
534 *Bacteroidota* and *Actinobacteria* (including *Bifidobacterium*) engraft very highly within the intestine
535 following faecal microbiota transplantation[32]. This highlights the possible role of *Bifidobacterium* and
536 *Bacteroides* in decolonising CRE-positive patients following faecal microbiota transplantation.
537
538 Polysaccharides, proteins, and mucins are major food sources for the gut microbiota in the large
539 intestine. Primary degraders break down these complex substrates, resulting in the extracellular
540 release of breakdown products (oligosaccharides, disaccharides, monosaccharides, peptides, and
541 amino acids)[15]. These simple compounds can support the growth of secondary degraders.
542 *Bacteroides* are important primary degraders (but can also degrade simple compounds) and
543 *Bifidobacterium* are important secondary degraders in the gut[33]. Therefore, this supports the
544 observation that decreases in the abundance of these bacteria following antibiotics results in an
545 enrichment of simple nutrients.
546
547 The nutrient-niche hypothesis predicts that expansion of *Enterobacteriaceae* in an antibiotic-
548 disrupted gut microbiota is due to an increase in the availability of nutrients, where competition for
549 these nutrients would normally restrict *Enterobacteriaceae* growth[14]. We demonstrated that
550 antibiotics (that promote susceptibility to CRE) increased the availability of nutrients that can support
551 CRE expansion within the gut. The monosaccharides, disaccharides, and amino acids of interest in
552 this study were derived from the breakdown of complex polysaccharides, proteins, and mucin,
553 including starch (glucose, maltose, trehalose)[34-37], inulin (fructose, glucose, sucrose)[38], pectin

554 (glucose, arabinose, galactose, xylose, mannose, fucose)[39], xylan (xylose, arabinose)[40],
555 arabinogalactan (arabinose, galactose)[41], mucin (N-acetylglucosamine, galactose, fucose, amino
556 acids)[42], peptone (amino acids)[43,44], and yeast extract (amino acids, ribose, uracil)[45]. Our results led
557 us to conclude that CRE have a growth advantage in antibiotic-perturbed gut microbiota by acting
558 as secondary fermenters of monosaccharides, disaccharides, and amino acids, highlighting the
559 important role of microbial cross-feeding in antibiotic-disrupted gut microbiota.
560
561 Previous studies demonstrated that antibiotics could enrich nutrients to support the growth of
562 intestinal pathogens. Cefoperazone (which promoted *Clostridioides difficile* intestinal colonisation)
563 increased nutrients (mannitol, fructose, sorbitol, raffinose, stachyose, and some amino acids) and
564 decreased metabolites (valerate and isovalerate) in the caecal microbiota of mice[46]. *In vitro*
565 experiments demonstrated that these nutrients supported *C. difficile* growth. Another study
566 demonstrated that sialic acid was increased in the caecal microbiota of mice treated with antibiotics
567 that promote susceptibility to *Salmonella enterica* serovar Typhimurium or *C. difficile*[10]. *S.*
568 Typhimurium and *C. difficile* mutants that were unable to utilise sialic acid showed impaired growth
569 within the intestine. In this study we found an enrichment of nutrients associated with
570 polysaccharides, mucin, and proteins, indicating that antibiotics cause a disruption of secondary
571 fermentation in the gut, where enrichment of these simple nutrients can support CRE growth.
572
573 Oxygen is a limiting resource for *Enterobacteriaceae* in the gut, and oxygenation of the gut that
574 occurs following antibiotics has been hypothesised to drive the expansion of *Enterobacteriaceae*[14].
575 Our results demonstrate that an increase in oxygen availability results in an increase in CRE growth
576 on nutrients that were enriched with antibiotics (compared to growth under anaerobic conditions).
577 This observation is supported by a recent longitudinal shotgun metagenomics sequencing analysis
578 of stool from CRE-positive patients which showed that aerobic respiration and oxidative
579 phosphorylation pathways (e.g. the pentose phosphate pathway) were enriched during CRE
580 colonisation (where antibiotic usage was common)[31]. Rivera-Chávez and colleagues demonstrated
581 that antibiotic treatment led to increased gut oxygenation that resulted in the aerobic expansion of
582 *S.* Typhimurium, demonstrating the advantage that oxygen can provide to facultatively anaerobic

583 pathogens[47]. Overall, our work supports the hypothesis that CRE growth is enhanced on carbon and
584 nitrogen sources (that become available due to antibiotic treatment) in the presence of oxygen.
585
586 The metabolism of monosaccharides and disaccharides produces SCFAs and the metabolism of
587 amino acids produces SCFAs and BCFAs[15,48]. We demonstrated that antibiotic treatment of the
588 faecal microbiota results in the disruption of nutrient metabolism, leading to the development of a
589 metabolite depleted environment. We showed that formate, acetate, propionate, butyrate, valerate,
590 isobutyrate, isovalerate, lactate, 5-aminovalerate, and ethanol were decreased by antibiotics.
591 *Bifidobacterium*, *Bacteroides*, and *Collinsella* (taxa that were decreased with antibiotics) are known
592 to produce many of these metabolites. *Bifidobacterium* produces acetate, lactate, ethanol, and
593 formate[15,49]. *Bacteroides* produces acetate, propionate, lactate, formate, ethanol, isobutyrate, and
594 isovalerate[15,50]. *Collinsella* produces ethanol, formate, and lactate[51].
595
596 We showed that a mixture of these 10 metabolites was inhibitory against CRE at pH values
597 representative of the human large intestine (pH 6, 6.5, and 7). However, the metabolite mixture was
598 more inhibitory at pH 6 and 6.5 compared to pH 7. Our work is supported by a previous study by
599 Sorbara and colleagues that demonstrated that acetate, propionate, and butyrate were decreased
600 in caecal content from mice treated with ampicillin[16]. They showed that a mixture of acetate,
601 propionate, and butyrate inhibited CRE growth at pH 5.75 (the pH of the mouse cecum) but not pH
602 7. It is possible that we observed higher levels of inhibition in the metabolite mixture at pH 7 due to
603 the inclusion of additional inhibitory metabolites in the mixture. This is supported by previous
604 observations that valerate can inhibit the growth of *C. difficile* at pH 7[7].
605
606 We demonstrated that 7 microbial metabolites (acetate, propionate, butyrate, valerate, isobutyrate,
607 isovalerate, and ethanol) inhibit CRE growth. Future research is required to solve the mechanisms
608 that these inhibitory metabolites use to inhibit intestinal CRE colonisation. It is unclear whether these
609 metabolites may act using one mechanism of inhibition or whether they may mediate inhibition by
610 multiple different mechanisms. We saw differences in the metabolites that inhibited *E. coli*, *K.*
611 *pneumoniae*, and *E. cloacae* growth, and it is not clear whether there are differences in the

612 mechanisms in these three different species. It is also unclear whether these metabolites may have
613 synergistic inhibitory effects, or whether these mechanisms may be impacted by different gut
614 environmental conditions. Future studies are needed to investigate how these metabolites impact
615 pathogens, other members of the gut microbiota, and the host to provide colonisation resistance
616 against CRE.
617
618 In this study we investigated the impact of microbial metabolites on the growth of CRE isolates.
619 However, it is important to further investigate the impact of microbial metabolites on the host, as this
620 may also impact the development of invasive CRE infections. For example, both butyrate and
621 valerate have been demonstrated to improve gut barrier integrity[52,53]. Therefore, a depletion of these
622 metabolites following antibiotic treatment may promote the translocation of CRE from the gut to the
623 bloodstream.
624
625 In summary, we provide evidence that antibiotics create an intestinal niche that supports CRE
626 expansion by enriching for nutrients that support CRE growth and by depleting metabolites that are
627 inhibitory towards CRE growth. Understanding how antibiotics disrupt colonisation resistance
628 against CRE is critical for the rational design of microbiome therapeutics that prevent or treat CRE
629 intestinal colonisation. These microbiome therapeutics could reduce the risk of patients developing
630 invasive CRE infections, reduce the recurrence of invasive CRE infections in chronically colonised
631 patients, and reduce the spread of CRE to susceptible patients. A second-generation microbiome
632 therapeutic may be composed of gut commensals that can outcompete CRE for nutrients and
633 convert them into inhibitory metabolites. A third-generation microbiome therapeutic may be
634 composed of a metabolite or mixture of metabolites that inhibit CRE growth, which could be
635 administered to CRE colonised patients while they are receiving antibiotic treatment.
636
637 In the short term, our results could be used to help reduce the risk of patients becoming colonised
638 with CRE. Our data could guide the prescription of antibiotics whereby clinicians avoid prescribing
639 antibiotics that elevate specific nutrients that support CRE growth and deplete specific metabolites
640 that inhibit CRE growth. Our data could also be used to identify patients that are at particular risk for

641 CRE intestinal colonisation by screening faecal samples for these nutrients and metabolites.

642

643 **MATERIALS AND METHODS**

644

645 ***Carbapenem-resistant* Enterobacteriaceae *isolates:***

646

647 New Delhi Metallo-β-lactamase 1 (NDM-1) *E. coli*, NDM-1 *K. pneumoniae*, and NDM-1 *E. cloacae*
648 were isolated from patients with intestinal CRE colonisation from the Imperial College Healthcare
649 NHS Trust (London, UK) via rectal swab (with approval from the London - Queen Square Research
650 Ethics Committee, 19/LO/0112). The species were classified by matrix assisted laser desorption
651 ionisation-time of flight mass spectrometry and later confirmed with 16S rRNA gene sequencing and
652 whole genome sequencing. CRE status was determined using X-pert Carba-R PCR detection
653 (Cepheid, Sunnyvale, CA)[54]. Genome sequencing data for these isolates have been deposited into
654 the European Nucleotide Archive under the project accession number PRJEB60914 and strains are
655 available upon request.

656

657 We also tested NDM-4 *E. coli* ST167 (NCTC 14333), OXA-48 *E. coli* ST410 (NCTC 14324), KPC-3
658 *K. pneumoniae* ST258 (NCTC 13438), and KPC-3 *K. pneumoniae* ST11 (NCTC 14327) as these are
659 prevalent clonal groups that are responsible for the rapid emergence of CRE clinical isolates
660 worldwide.[55]

661

662 ***Ethical approval:***

663

664 Ethical approval was received by the London - Queen Square Research Ethics Committee
665 (19/LO/0112) and the South Central - Oxford C Research Ethics Committee (16/SC/0021 and
666 20/SC/0389) to collect faecal samples from human donors. Faecal donors were healthy human
667 donors aged between 18-65 years old and had not received antibiotic treatment in the 6+ months
668 prior to donation. Informed consent was obtained from human participants.

669

670 ***Faecal culture experiments:***

671

672 We performed *ex vivo* faecal culture experiments to measure the effects of eight broad-spectrum
673 antibiotics on the faecal microbiota collected from 11 healthy human donors (6 males, 5 females).
674 Female faecal donors were 33.2 ± 16.0 years old and male faecal donors were 29.7 ± 6.4 years old.
675 Faecal culture experiments were performed under anaerobic conditions using a standardised distal
676 gut growth medium mimicking nutrients found in the distal gut, including polysaccharides, proteins,
677 and mucin[56]. For each donor, fresh faeces were inoculated into the distal gut growth medium at a
678 2% (w/v) concentration. Faecal cultures were supplemented with water (antibiotic-naïve control) or
679 one of the following antibiotics (at concentrations measured in faeces): 2 µg/ml MEM, 2 µg/ml IPM,
680 37 µg/ml ETP, 139 µg/ml TZP, 152 µg/ml CRO, 22 µg/ml CAZ, 2 µg/ml CTX, 139 µg/ml CIP[18,26-28,57-
681 60]. These antibiotics are known to promote the intestinal colonisation with CRE and are used
682 frequently in routine clinical practice[5]. Faecal cultures were run in triplicate and incubated
683 anaerobically at 37°C for 24 hours. Samples were analysed by proton nuclear magnetic resonance
684 (^{1}H-NMR) spectroscopy (for nutrient and metabolite profiling) and 16S rRNA gene sequencing with
685 16S rRNA gene qPCR (for bacterial composition and biomass).

686

687 A second set of *ex vivo* faecal culture experiments was performed to measure the CRE growth in
688 TZP-treated and antibiotic-naïve faecal microbiota. Faecal samples were donated from 5 healthy
689 human donors (2 males, 3 females), and these faecal samples were separate from the faecal
690 samples collected above. Female faecal donors were 31.3 ± 5.5 years old and male faecal donors
691 were 31.0 ± 9.9 years old. For each donor, fresh faeces were inoculated into the distal gut growth
692 medium supplemented with TZP (139 µg/ml) or water and spiked with 10^3 CFU/ml one of the
693 following CRE isolates: NDM-1 *E. coli*, NDM-4 *E. coli* (ST167), OXA-48 *E. coli* (ST410), KPC-3 *K.*
694 *pneumoniae* (ST258), or KPC-3 *K. pneumoniae* (ST11). Faecal cultures were run in duplicate and
695 incubated anaerobically at 37°C for 24 hours. Samples were plated on Brilliance CRE agar to
696 quantify CRE growth.

697

698 ***16S rRNA gene sequencing and 16S rRNA gene qPCR:***

699

700 DNA was extracted from 250 µl of faecal culture sample using the DNeasy PowerLyzer PowerSoil
701 Kit (Qiagen, Germany) according to manufacturer's instructions, with the addition of a bead beating
702 step for 3 minutes at speed 8 in a Fast-Prep 24 bead beater (MP Biomedicals, USA). DNA was
703 stored at -80°C until it was ready to be used.

704

705 Illumina's 16S metagenomic sequencing library preparation protocol was used to generate sample
706 libraries amplifying the V1-V2 regions of the 16S rRNA gene, as previously described[61]. The
707 SequalPrep Normalisation Plate Kit (Life Technologies, UK) was used to clean up and normalise the
708 index PCR reactions. The NEBNext Library Quant Kit for Illumina (New England Biolabs, UK) was
709 used to quantify sample libraries. Sample libraries were sequenced on an Illumina MiSeq platform
710 (Illumina Inc., UK) using the MiSeq Reagent Kit v3 (Illumina) and paired-end 300bp chemistry. 16S
711 rRNA gene qPCR was performed to quantify the bacterial biomass as previously described[7].

712

713 16S rRNA gene sequencing data were imported into R and processed using the standard DADA2
714 pipeline (version 1.18.0)[62]. The SILVA bacterial database version 138.1 was used to classify the
715 sequence variants. 16S rRNA gene sequencing data was expressed as absolute abundances using
716 the 16S rRNA gene qPCR data, as previously described[7].

717

718 ***^{1}H-NMR spectroscopy:***

719

720 Supernatants were prepared from human faeces by vortexing 300 mg of faeces in 900 µl of high-
721 performance liquid chromatography-grade water for 10 minutes at 3000 rpm followed by
722 centrifugation at 17,000 × g for 10 minutes at 4°C. Supernatants were prepared from faecal culture
723 samples by centrifugation at 17,000 × g for 10 minutes at 4°C. Supernatants were prepared from
724 mouse faeces by vortexing 20 mg of faeces in 560 µl of high-performance liquid chromatography-
725 grade water for 10 minutes at 3000 rpm followed by centrifugation at 17,000 × g for 10 minutes at
726 4°C.

727

728 ^{1}H-NMR spectroscopy was performed as previously described[7]. Briefly, sample supernatants were
729 randomised and defrosted at room temperature for 1 hour. Sample supernatants were centrifuged
730 for 10 min at 17,000 × g and 4°C and the pellet was discarded. For human faeces and faecal batch
731 culture samples, 400 µl of supernatant was added to 250 µl NMR buffer (28.85 g Na_2HPO_4, 5.25 g
732 NaH_2PO_4, 1 mM 3-(Trimethylsilyl)propionic-2,2,3,3-d_4 acid sodium salt (TSP), 3 mM NaN_3, deuterium
733 oxide to 1 L, pH 7.4). For mouse faecal samples 540 µl of supernatant was added to 60 µl NMR
734 buffer (20.4 g KH_2PO_4, 5.8 mM TSP, 2 mM NaN_3, deuterium oxide to 100 mL, pH 7.4). Each 5 mm
735 NMR tube was filled with 600 µl of sample and loaded into the SampleJet system.

736

737 ^{1}H-NMR spectroscopy was performed using the Bruker AVANCE III HD 800 MHz spectrometer
738 (Bruker Bio-Spin, Rheinstetten, Germany) using a 5mm CPTCI 1H-13C/15N/D Z-gradient cryoprobe.
739 1D spectra (a standard NOESYGPPR1D pulse sequence (RD-90°-t1-90°-tm-90°-ACQ)) as well as
740 2D spectra (standard 2D JRESGPPRQF pulse sequence) were acquired. A recycle delay of 4
741 seconds and mixing time of 100 ms was used. The 90° pulse length was approximately 10 µs. For
742 the human faecal samples and faecal batch culture samples 32 scans were recorded. For the mouse
743 faecal samples 128 scans were recorded.

744

745 NMR spectra underwent auto processing, which includes exponential window function (line
746 broadened by 0.3 Hz), auto phasing (zero-order), auto baseline correction, and auto referencing.
747 NMR spectra were imported into MATLAB r2019b (The Mathworks, USA) using a custom script.
748 Spectra were aligned and the water (4.6 – 5 ppm) and TSP (-0.2 – 0.2 ppm) peaks were cut.
749 Compounds were identified by comparison to spectral databases in Chenomx NMR Suite (Chenomx,
750 Canada). Representative peaks were integrated for quantification of compounds. A signal-to-noise
751 ratio cut-off value of 3:1 was used to define the limit of detection for peak detection.[63] The minimal
752 signal-to-noise ratio was 6.1:1 for the 32 scan human faecal dataset, 3.8:1 for the 32 scan faecal
753 batch culture dataset, and 4.0:1 for the 123 scan mouse faecal dataset.

754

755 ***mixOmics analysis:***

756

757 rCCA modelling was used to correlate 16S rRNA gene sequencing data (family level) with ^{1}H-NMR
758 data for faecal cultures samples using the *mixOmics* library within R, as previously described[7,21]. In
759 unit representation plots each point represents a single faecal culture sample that was projected into
760 the XY-variate space. In the correlation circle plots features projected in the same direction from the
761 origin have a positive correlation, and features projected in opposite directions from the origin have
762 a negative correlation. Features sitting at farther distances from the origin have stronger correlations
763 than features sitting closer to the origin.

764

765 ***Carbon and nitrogen utilisation assays:***

766

767 Compounds that were enriched in antibiotic-treated faecal microbiota were tested as nutrients in
768 growth assays to determine whether they could act as carbon or nitrogen sources to support CRE
769 growth. Growth of CRE isolates on sole carbon or nitrogen sources were tested by inoculating each
770 CRE isolate into a minimal medium supplemented with the nutrient of interest. First, CRE isolates
771 were passaged from frozen glycerol stocks onto R2A plates. Cells were suspended in M9 minimal
772 media to a turbidity of 42% using a Turbidimeter (Biolog Inc., Hayward, CA), then further diluted 1 in
773 6 to inoculate the carbon or nitrogen utilisation assays. M9 minimal media contained the following
774 (at final concentrations): 22 mM KH_2PO_4, 42 mM Na_2HPO_4, 9 mM NaCl, 0.49 mM $MgSO_4{\bullet}7H_2O$,
775 0.09 mM $CaCl_2$, 0.011 mM $FeSO_4{\bullet}7H_2O$. For the carbon assays the M9 minimal medium was also
776 supplemented with 0.1% (w/v) NH_4Cl (as the nitrogen source) and the carbon sources were
777 individually tested at 0.5% (w/v) concentration. For the nitrogen assays the M9 minimal medium was
778 also supplemented with 0.5% (w/v) glucose (as the carbon source) and the nitrogen sources were
779 individually tested at 0.1% (w/v) concentration. Cultures were incubated anaerobically and
780 aerobically in a plate reader and optical density (OD_{600}) readings were collected every 15 minutes
781 for 24 hours.

782

783 ***Mixed nutrient preference assays:***

784

785 CRE isolates were passaged from frozen glycerol stocks on R2A plates. Cells were suspended in
786 M9 minimal media to a turbidity of 42% using a Turbidimeter, and then further diluted 1 in 6 to
787 inoculate the nutrient preference assays. M9 minimal media was supplemented with 0.015% (w/v)
788 of each of the following nutrients (as the sole carbon and nitrogen sources): L-arabinose, D-fructose,
789 L-fucose, D-galactose, D-glucose, D-mannose, D-ribose, D-xylose, N-acetylglucosamine, D-
790 maltose, sucrose, D-trehalose, L-alanine, L-arginine, L-aspartate, L-glutamate, L-glycine, L-
791 isoleucine, L-leucine, L-lysine, L-methionine, L-phenylalanine, L-proline, L-threonine, L-tryptophan,
792 L-tyrosine, L-valine, uracil, and succinate. Cultures were incubated anaerobically and aerobically in
793 a plate reader and OD_{600} readings were collected every 15 minutes for 24 hours. Cultures were also
794 incubated anaerobically and aerobically for 24 h and samples were collected at 0, 4, 8, and 24 hours
795 post-inoculation for ^{1}H-NMR spectroscopy. The starting nutrient concentration was measured by the
796 integration of a representative peak in the NMR spectrum from samples collected at 0 hours and this
797 concentration was set to 100% to enable measurements of percent nutrient remaining at 4, 8, and
798 24 hours.
799
800 ***Analysis of Microbial Growth Assays (AMiGA):***
801
802 Growth curves were analysed in Python (v3.6.5) using the AMiGA software[64]. Growth of each isolate
803 was measured with 6 replicates from 2-3 independent experiments. Growth curves were normalised
804 to the no substrate control using the subtraction method. AMiGA performed Gaussian Process
805 regression to test differential growth between the substrate and the no substrate control. The
806 functional difference in the OD_{600} (and its credible interval) was also computed between the substrate
807 and the no substrate control.
808
809 ***Metabolite measurements from healthy human faeces:***
810
811 The concentration of 10 microbial metabolites were measured from the faeces of 12 healthy human
812 donors (5 males, 7 females) by ^{1}H-NMR spectroscopy. This was a separate set of faecal samples
813 than the faecal samples that were used to inoculate the faecal culture experiments. Female faecal

814 donors were 30.9 ± 12.1 years old and male donors were 27.8 ± 5.3 years old. Metabolite
815 concentrations were measured from NMR spectra using the Chenomx NMR Suite (v8.6). **Table S2**
816 shows the approximate minimum, average, and maximum concentrations of each metabolite that
817 was tested in the metabolite inhibition assays, which were based on the measurements of the
818 microbial metabolites from the healthy donor faeces.
819
820 ***Mixed metabolite inhibition assay:***
821
822 Microbial metabolites that were present in antibiotic-naïve faecal microbiota but depleted in
823 antibiotic-treated faecal microbiota were tested as potential inhibitory compounds in growth assays.
824 We tested whether a mixture of microbial metabolites (that were decreased in antibiotic-treated
825 faecal microbiota) would be able to inhibit the growth of each CRE isolate. The metabolite mixture
826 was composed of formate, acetate, propionate, butyrate, valerate, isobutyrate, isovalerate, lactate,
827 5-aminovalerate, and ethanol. Each metabolite was added to the mixture at a concentration that
828 mimicked the average concentration measured in healthy human faecal samples (**Table S2**). Luria
829 broth (LB) was supplemented with the metabolite mixture and compared to a no metabolite control.
830 Overnight cultures of each CRE isolate were inoculated into the supplemented LB at 10^3 CFU/ml.
831 The assay was run at pH 6, 6.5, and 7 to mimic the pH range found in healthy faeces[23,65]. Cultures
832 were incubated anaerobically for 16 hours at 37°C. Growth was measured at OD_{600} after 16 hours
833 of incubation.
834
835 We also measured the growth of CRE isolates in LB supplemented with a mixture of acetate,
836 propionate, butyrate, and valerate. Each metabolite was added to the mixture at a concentration that
837 mimicked the average concentration measured in healthy human faecal samples (**Table S2**). LB was
838 supplemented with the metabolite mixture and compared to a no metabolite control. The assay was
839 run at pH 6.5. Overnight cultures of each CRE isolate were inoculated into the supplemented LB at
840 10^3 CFU/ml. Cultures were incubated anaerobically for 16 hours at 37°C. Growth was measured at
841 OD_{600} after 16 hours of incubation.
842

843 ***Individual metabolite inhibition assay:***

844

845 We next tested whether individual microbial metabolites (that were decreased in antibiotic-treated
846 faecal microbiota) would be able to inhibit the growth of each CRE isolate. The individual metabolites
847 tested included formate, acetate, propionate, butyrate, valerate, isobutyrate, isovalerate, lactate, 5-
848 aminovalerate, and ethanol. Each metabolite was tested at three concentrations that mimicked the
849 low, average, and high concentrations measured in healthy human faecal samples (**Table S2**). LB
850 was supplemented with each metabolite and compared to a no metabolite control. Overnight cultures
851 of each CRE isolate were inoculated into the supplemented LB at 10^3 CFU/ml. The assay was run
852 at pH 6.5 as this was representative of the distal gut and showed inhibition in the mixed metabolite
853 assay. Cultures were incubated anaerobically for 16 hours at 37°C. Growth was measured at OD_{600}
854 after 16 hours of incubation.

855

856 ***Mouse model of intestinal colonisation with carbapenem-resistant* E. coli*:***

857

858 Ethical approval for mouse experiments was received from the Imperial College London Animal
859 Welfare and Ethical Review Body (PF93C158E) and performed under the authority of the UK Home
860 Office, as described in the Animals (Scientific Procedures) Act 1986. We abided by standards
861 outlined in the Animal Research: Reporting of In Vivo Experiments (ARRIVE) guidelines.

862

863 Eight- to ten-week-old female wild-type C57BL/6 mice (purchased from Envigo, Huntingdon, UK)
864 were acclimatised for 1 week prior to the start of the experiment. Each test group contained 5 mice
865 that were housed 5 per cage (in individually ventilated cages). Mice were provided autoclaved food
866 (RM1, Special Diet Services, Essex, UK), water (provided ad libitum), and bedding (Aspen chip 2
867 bedding, NEPCO, Warrensburg, New York). Mice were maintained at 20–22°C in a 12-hour light
868 and 12-hour dark cycle (all interventions were performed during the light cycle).

869

870 We performed a mouse experiment to measure changes in nutrient availability in mouse faeces
871 following TZP treatment and NDM-1 *E. coli* colonisation, and to measure NDM-1 *E. coli* growth in

872 mouse faeces following the administration of a mixture of inhibitory metabolites. We used a
873 previously published mouse model of intestinal CRE colonisation as described by Perez and
874 colleagues (**Figs. 7a and 9a**)[19]. The dosing schedule of the metabolite mixture was designed based
875 on a previous study from our group, where we investigated the effects of the microbial metabolite
876 valerate on the intestinal colonisation with *Clostridioides difficile* in a mouse model.[7]
877
878 In this study, mice were subcutaneously administered 8 mg of TZP (in 0.2 ml saline) or 0.2 ml of
879 saline once per day for 5 days to mimic the daily TZP dose recommended for human adults[19]. On
880 the third day of TZP or saline administration, 10^6 CFU of carbapenem-resistant (NDM-1) *E. coli*
881 (diluted in 0.2 ml saline) were orally administered to the mice. Next, TZP-treated mice that were
882 colonised with *E. coli* were fed by oral gavage with 0.2 ml of a mixture of metabolites (glycerol
883 triacetate, 65 mM; glycerol tripropionate, 15 mM; glycerol tributyrate, 15 mM; and glycerol trivalerate,
884 3.5 mM; diluted in PBS) or 0.2 ml of PBS once per day for 3 days. Faecal samples were collected
885 for NDM-1 *E. coli* plate counts (on Brilliance CRE agar, Oxoid, Basingstoke, UK) and for ^{1}H-NMR
886 spectroscopy.
887
888 ***Statistical analysis:***
889
890 Statistical tests were performed using IBM SPSS Statistics Software 27 (IBM Corp, Armonk, New
891 York), GraphPad Prism 9.4.1 (La Jolla, California), or in R (v4.2.2). A p value less than 0.05 was
892 considered significant. 16S rRNA gene sequencing data (weighted as absolute abundances) were
893 analysed using Wilcoxon signed rank test with Benjamini & Hochberg FDR correction using the
894 DA.wil function within in the DAtest R package version 2.7.18. Peak integration values from the ^{1}H-
895 NMR data were analysed using Wilcoxon signed rank test with Benjamini & Hochberg FDR
896 correction using the DA.wil function within in the DAtest R package version 2.7.18 or a paired t-test
897 (two-sided) with Benjamini & Hochberg FDR correction using the pairwise_t_test function within the
898 rstatix R package version 0.7.1. A Mann-Whitney U test was used to compare log10-transformed
899 CRE counts from TZP-treated faecal cultures compared to water-treated faecal cultures.
900 Regularised canonical correlation analysis (rCCA) was used to correlate the 16S rRNA gene

901 sequencing data and ^{1}H-NMR data using the mixOmics library within R (as described above)[7,21]. For
902 the carbon and nitrogen utilisation assays the growth curves were analysed in Python (v3.6.5) using
903 the AMiGA software (as described above)[64]. For the nutrient preference experiment changes in the
904 concentration of nutrients and metabolites for each CRE isolate were compared to the sterile media
905 control over time using a two-way mixed ANOVA followed by pairwise comparisons with Bonferroni
906 correction. For the *in vitro* mixed metabolite inhibition test, growth of the CRE isolate in the metabolite
907 mixture was compared to growth in the no metabolite control at each pH using an unpaired t-test
908 (two-sided). For the *in vitro* individual metabolite inhibition test, growth of the CRE isolate in the
909 presence of each metabolite was compared to the no metabolite control using a one-way ANOVA
910 followed by Dunn's multiple comparison test. For the mouse experiments, a paired t-test (two-sided)
911 or a Mann-Whitney U test was used to compare log10-transformed NDM-1 *E. coli* counts from the
912 faecal pellets of metabolite-treated mice compared to PBS-treated mice.
913
914 **REFERENCES:**

915 1. Dadgostar, P. Antimicrobial resistance: implications and costs. *Infect Drug Resist* **12**, 3903-3910
916 (2019).
917 2. Ventola, C. L. The antibiotic resistance crisis: part 1: causes and threats. *P T* **40**, 277-83 (2015).
918 3. Manges, A. R., Steiner, T. S. & Wright, A. J. Fecal microbiota transplantation for the intestinal
919 decolonization of extensively antimicrobial-resistant opportunistic pathogens: a review. *Infect.*
920 *Dis. (Lond)* **48**, 587-592 (2016).
921 4. Kim, S., Covington, A. & Pamer, E. G. The intestinal microbiota: Antibiotics, colonization
922 resistance, and enteric pathogens. *Immunol Rev* **279**, 90-105 (2017).
923 5. UK Health Security Agency. Framework of actions to contain carbapenemase-producing
924 Enterobacterales. *UK Health Security Agency*
925 https://assets.publishing.service.gov.uk/government/uploads/system/uploads/attachment_data
926 /file/1107705/Framework_of_actions_to_contain_CPE.pdf (2022).
927 6. Reed, A. D. & Theriot, C. M. Contribution of inhibitory metabolites and competition for nutrients to
928 colonization resistance against *Clostridioides difficile* by commensal *Clostridium*.
929 *Microorganisms* **9**, 371 (2021).

930 7. McDonald, J. A. K. *et al*. Inhibiting growth of *Clostridioides difficile* by restoring valerate, produced
931 by the intestinal microbiota. *Gastroenterology* **155**, 1495-1507 (2018).
932 8. Jacobson, A. *et al*. A gut commensal-produced metabolite mediates colonization resistance to
933 *Salmonella* infection. *Cell. Host Microbe* **24**, 296-307.e7 (2018).
934 9. Ferreyra, J. A. *et al*. Gut microbiota-produced succinate promotes *C. difficile* infection after
935 antibiotic treatment or motility disturbance. *Cell. Host Microbe* **16**, 770-777 (2014).
936 10. Ng, K. M. *et al*. Microbiota-liberated host sugars facilitate post-antibiotic expansion of enteric
937 pathogens. *Nature* **502**, 96-99 (2013).
938 11. Pudlo, N. A. *et al*. Phenotypic and genomic diversification in complex carbohydrate-degrading
939 human gut bacteria. *mSystems* **7**, e0094721 (2022).
940 12. Chang, D. E. *et al*. Carbon nutrition of *Escherichia coli* in the mouse intestine. *PNAS USA* **101**,
941 7427-32 (2004).
942 13. Tuncil, Y. E. *et al*. Reciprocal prioritization to dietary glycans by gut bacteria in a competitive
943 environment promotes stable coexistence. *mBio* **8**, 1068 (2017).
944 14. Rivera-Chávez, F., Lopez, C. A. & Bäumler, A. J. Oxygen as a driver of gut dysbiosis. *Free Radic*
945 *Biol Med* **105**, 93-101 (2016).
946 15. Oliphant, K. & Allen-Vercoe, E. Macronutrient metabolism by the human gut microbiome: major
947 fermentation by-products and their impact on host health. *Microbiome* **7**, 91 (2019).
948 16. Sorbara, M. T. *et al*. Inhibiting antibiotic-resistant *Enterobacteriaceae* by microbiota-mediated
949 intracellular acidification. *J. Exp. Med.* **216**, 84-98 (2019).
950 17. Djukovic, A. *et al*. *Lactobacillus* supports *Clostridiales* to restrict gut colonization by multidrug-
951 resistant *Enterobacteriaceae*. *Nat Commun* **13**, 5617 (2022).
952 18. Ladirat, S. E. *et al*. High-throughput analysis of the impact of antibiotics on the human intestinal
953 microbiota composition. *J Microbiol Methods* **92**, 387-97 (2013).
954 19. Perez, F., Pultz, M. J., Endimiani, A., Bonomo, R. A. & Donskey, C. J. Effect of antibiotic
955 treatment on establishment and elimination of intestinal colonization by KPC-producing
956 *Klebsiella pneumoniae* in mice. *Antimicrob Agents Chemother* **55**, 2585–2589 (2011).

957 20. Venturini, C., Bowring, B., Fajardo-Lubian, A., Devine, C. & Iredell, J. Effects of antibiotic
958 treatment with piperacillin/tazobactam versus ceftriaxone on the composition of the murine gut
959 microbiota. *Antimicrob Agents Chemother* **65**, 1504 (2021).
960 21. K. Le Cao, F. Rohart, I. Gonzalez and S. Dejean. mixOmics: Omics Data Integration Project. R
961 package version 6.1.2. https://bioconductor.org/packages/mixOmics/ (2017).
962 22. Autieri, S. M. *et al*. L-fucose stimulates utilization of D-ribose by *Escherichia coli* MG1655
963 DeltafucAO and *E. coli* Nissle 1917 DeltafucAO mutants in the mouse intestine and in M9
964 minimal medium. *Infect Immun* **75**, 5465-75 (2007).
965 23. Shelton, C. D. *et al*. *Salmonella enterica* serovar Typhimurium uses anaerobic respiration to
966 overcome propionate-mediated colonization resistance. *Cell Rep* **38**, 110180 (2022).
967 24. Schwartz, B. The effect of temperature on the rate of hydrolysis of triglycerides by pancreatic
968 lipase. *J. Gen. Physiol.* **27**, 113-118 (1943).
969 25. Bergan, T., Nord, C. E. & Thorsteinsson, S. B. Effect of meropenem on the intestinal microflora.
970 *Eur J Clin Microbiol Infect Dis* **10**, 524-7 (1991).
971 26. Kager, L., Brismar, B., Malmborg, A. S. & Nord, C. E. Imipenem concentrations in colorectal
972 surgery and impact on the colonic microflora. *Antimicrob Agents Chemother* **33**, 204-8 (1989).
973 27. Pletz, M. *et al*. Ertapenem pharmacokinetics and impact on intestinal microflora, in comparison
974 to those of ceftriaxone, after multiple dosing in male and female volunteers. *Antimicrob Agents*
975 *Chemother* **48**, 3765-72 (2004).
976 28. Nord, C. E., Brismar, B., Kasholm-Tengve, B. & Tunevall, G. Effect of piperacillin/tazobactam
977 treatment on human bowel microflora. *J Antimicrob Chemother* **31**, 61-5 (1993).
978 29. Stewardson, A. J. *et al*. Collateral damage from oral ciprofloxacin versus nitrofurantoin in
979 outpatients with urinary tract infections: a culture-free analysis of gut microbiota. *Clin Microbiol*
980 *Infect* **21**, 344.e1-11 (2015).
981 30. Guk, J. *et al*. Modeling the bacterial dynamics in the gut microbiota following an antibiotic-induced
982 perturbation. *CPT Pharmacometrics Syst Pharmacol* **11**, 906-918 (2022).
983 31. Kang, J. *et al*. Long-term ecological and evolutionary dynamics in the gut microbiomes of
984 carbapenemase-producing *Enterobacteriaceae* colonized subjects. *Nat Microbiol* **7**, 1516-1524
985 (2022).

986 32. Ianiro, G. *et al*. Variability of strain engraftment and predictability of microbiome composition after
987 fecal microbiota transplantation across different diseases. *Nat Med* **28**, 1913-1923 (2022).
988 33. Fernandez-Julia, P., Commane, D. M., van Sinderen, D. & Munoz-Munoz, J. Cross-feeding
989 interactions between human gut commensals belonging to the *Bacteroides* and *Bifidobacterium*
990 genera when grown on dietary glycans. *Microbiome Res Rep* **1**, 1-12 (2022).
991 34. DeMartino, P. & Cockburn, D. W. Resistant starch: impact on the gut microbiome and health.
992 *Curr Opin Biotechnol* **61**, 66-71 (2020).
993 35. Cerqueira, F. M., Photenhauer, A. L., Pollet, R. M., Brown, H. A. & Koropatkin, N. M. Starch
994 digestion by gut bacteria: crowdsourcing for carbs. *Trends Microbiol* **28**, 95-108 (2020).
995 36. Vital, M. *et al*. Metagenomic Insights into the degradation of resistant starch by human gut
996 microbiota. *Appl Environ Microbiol* **84**, 1562 (2018).
997 37. Chi, Z., Liu, J. & Zhang, W. Trehalose accumulation from soluble starch by *Saccharomycopsis*
998 *fibuligera* sdu. *Enzyme Microb Technol* **28**, 240-245 (2001).
999 38. Niness, K. R. Inulin and oligofructose: what are they? *J Nutr* **129**, 1402S-6S (1999).
1000 39. Kaya, M., Sousa, A. G., Crépeau, M. J., Sørensen, S. O. & Ralet, M. C. Characterization of citrus
1001 pectin samples extracted under different conditions: influence of acid type and pH of extraction.
1002 *Ann Bot* **114**, 1319-26 (2014).
1003 40. Bastawde, K. B. Xylan structure, microbial xylanases, and their mode of action. *World J Microbiol*
1004 *Biotechnol* **8**, 353-68 (1992).
1005 41. Kelly, G. S. Larch arabinogalactan: clinical relevance of a novel immune-enhancing
1006 polysaccharide. *Altern Med Rev* **4**, 96-103 (1999).
1007 42. Pultz, N. J., Hoskins, L. C. & Donskey, C. J. Vancomycin-resistant enterococci may obtain
1008 nutritional support by scavenging carbohydrate fragments generated during mucin degradation
1009 by the anaerobic microbiota of the colon. *Microb Drug Resist* **12**, 63-7 (2006).
1010 43. Smid, E. J., Poolman, B. & Konings, W. N. Casein utilization by lactococci. *Appl Environ Microbiol*
1011 **57**, 2447-52 (1991).
1012 44. Assaf, A. *et al*. Evaluation of the impact of buffered peptone water composition on the
1013 discrimination between *Salmonella enterica* and *Escherichia coli* by Raman spectroscopy. *Anal*
1014 *Bioanal Chem* **412**, 3595-3604 (2020).

1015 45. Raja Makendran Nandan Raja Rajendran. Enzymatic Conversion of RNA from Yeast Extract to
1016 Guanosine monophosphate (a flavoring agent). Master's thesis, Chalmers University of
1017 Technology https://odr.chalmers.se/handle/20.500.12380/166692 (2012).
1018 46. Theriot, C. M. *et al*. Antibiotic-induced shifts in the mouse gut microbiome and metabolome
1019 increase susceptibility to *Clostridium difficile* infection. *Nat. Commun.* **5**, 3114 (2014).
1020 47. Rivera-Chávez, F. *et al*. Depletion of butyrate-producing clostridia from the gut microbiota drives
1021 an aerobic luminal expansion of *Salmonella*. *Cell Host Microbe* **19**, 443-54 (2016).
1022 48. Mortensen, P. B., Holtug, K. & Rasmussen, H. S. Short-chain fatty acid production from mono-
1023 and disaccharides in a fecal incubation system: implications for colonic fermentation of dietary
1024 fiber in humans. *J Nutr* **118**, 321-5 (1988).
1025 49. Van der Meulen, R., Adriany, T., Verbrugghe, K. & De Vuyst, L. Kinetic analysis of bifidobacterial
1026 metabolism reveals a minor role for succinic acid in the regeneration of NAD+ through its growth-
1027 associated production. *Appl Environ Microbiol* **72**, 5204-10 (2006).
1028 50. Rios-Covian, D., Salazar, N., Gueimonde, M. & de Los Reyes-Gavilan, C G. Shaping the
1029 metabolism of intestinal *Bacteroides* population through diet to improve human health. *Front*
1030 *Microbiol* **8**, 376 (2017).
1031 51. Kageyama, A., Benno, Y. & Nakase, T. Phylogenetic and phenotypic evidence for the transfer of
1032 *Eubacterium aerofaciens* to the genus *Collinsella* as *Collinsella aerofaciens* gen. nov., comb.
1033 nov. *Int J Syst Bacteriol* **49**, 557-65 (1999).
1034 52. Ghosh, S., Whitley, C. S., Haribabu, B. & Jala, V. R. Regulation of intestinal barrier function by
1035 microbial metabolites. *Cell Mol Gastroenterol Hepatol* **11**, 1463-1482 (2021).
1036 53. Gao, G. *et al*. Effects of valerate on intestinal barrier function in cultured Caco-2 epithelial cell
1037 monolayers. *Mol Biol Rep* **49**, 1817-1825 (2022).
1038 54. Otter, J. A. *et al*. Detecting carbapenemase-producing *Enterobacterales* (CPE): an evaluation of
1039 an enhanced CPE infection control and screening programme in acute care. *J Antimicrob*
1040 *Chemother* **75**, 2670-2676 (2020).
1041 55. Kantele, A. *et al*. Dynamics of intestinal multidrug-resistant bacteria colonisation contracted by
1042 visitors to a high-endemic setting: a prospective, daily, real-time sampling study. *Lancet Microbe*
1043 **2**, e151-e158 (2021).

1044 56. McDonald, J. A. *et al*. Evaluation of microbial community reproducibility, stability and composition
1045 in a human distal gut chemostat model. *J. Microbiol. Methods* **95**, 167-174 (2013).
1046 57. Moon, Y. S., Chung, K. C. & Gill, M. A. Pharmacokinetics of meropenem in animals, healthy
1047 volunteers, and patients. *Clin Infect Dis* **24**, S249–S255 (1997).
1048 58. Burdet, C. *et al*. Ceftriaxone and cefotaxime have similar effects on the intestinal microbiota in
1049 human volunteers treated by standard-dose regimens. *Antimicrob Agents Chemother* **63**, 2244
1050 (2019).
1051 59. Pessôa de Menezes e Silva, C H. Elaboration and evaluation of a new screening medium for
1052 detection and presumptive identification of extended-spectrum beta-lactamase-producing
1053 organisms (ESBL). *Braz J Microbiol* **31**, 271-274 (2000).
1054 60. Brismar, B., Edlund, C., Malmborg, A. S. & Nord, C. E. Ciprofloxacin concentrations and impact
1055 of the colon microflora in patients undergoing colorectal surgery. *Antimicrob Agents Chemother*
1056 **34**, 481-3 (1990).
1057 61. Mullish, B. H. *et al*. Functional microbiomics: evaluation of gut microbiota-bile acid metabolism
1058 interactions in health and disease. *Methods* **149**, 49-58 (2018).
1059 62. Callahan, B. J. *et al*. DADA2: High-resolution sample inference from Illumina amplicon data. *Nat*
1060 *Methods* **13**, 581-3 (2016).
1061 63. Webb, A. Increasing the sensitivity of magnetic resonance spectroscopy and imaging. *Anal*
1062 *Chem* **84**, 9-16 (2012).
1063 64. Midani, F. S., Collins, J. & Britton, R. A. AMiGA: software for automated analysis of microbial
1064 growth assays. *mSystems* **6**, e0050821 (2021).
1065 65. Payne, A. N., Zihler, A., Chassard, C. & Lacroix, C. Advances and perspectives in *in vitro* human
1066 gut fermentation modeling. *Trends Biotechnol.* **30**, 17-25 (2012).